JAERI-M
86-051

ANNUAL REPORT OF THE OSAKA LABORATORY FOR RADIATION CHEMISTRY JAPAN ATOMIC ENERGY RESEARCH INSTITUTE (NO. 18)

April 1, 1984 - March 31, 1985

March 1986

Osaka Laboratory for Radiation Chemistry

日本原子力研究所
Japan Atomic Energy Research Institute

JAERI-Mレポートは，日本原子力研究所が不定期に公刊している研究報告書です。
入手の問合わせは，日本原子力研究所技術情報部情報資料課（〒319－11茨城県那珂郡東海村）あて，お申しこしください。なお，このほかに財団法人原子力弘済会資料センター（〒319-11茨城県那珂郡東海村日本原子力研究所内）で複写による実費頒布をおこなっております。

JAERI-M reports are issued irregularly.
Inquiries about availability of the reports should be addressed to Information Division, Department of Technical Information, Japan Atomic Energy Research Institute, Tokai-mura, Naka-gun, Ibaraki-ken 319-11, Japan.

編集兼発行　日本原子力研究所
印　　刷　日立高速印刷株式会社

昭和59度日本原子力研究所大阪支所年報（No.18）
1984年4月1日～1985年3月31日

日本原子力研究所高崎研究所大阪支所

（1986年2月13日受理）

本報告は，大阪支所において昭和59年度に行なわれた研究活動を述べたものである。主な研究題目は，電子及びイオン照射下の界面現象に関する基礎研究，電子線照射による重合反応の研究，ポリマーの改質及び上記の研究と関連して重合反応、高分子の分解及び架橋ならびにグラフト重合に関する基礎的研究などである。

日本放射線高分子研究協会年報	Vol. 1		1958／1959
日本放射線高分子研究協会年報	Vol. 2		1960
日本放射線高分子研究協会年報	Vol. 3		1961
日本放射線高分子研究協会年報	Vol. 4		1962
日本放射線高分子研究協会年報	Vol. 5		1963
日本放射線高分子研究協会年報	Vol. 6		1964
日本放射線高分子研究協会年報	Vol. 7		1965
日本放射線高分子研究協会年報	Vol. 8		1966
日本原子力研究所大阪研における放射線化学の基礎研究No.1	JAERI	5018	1967
日本原子力研究所大阪研における放射線化学の基礎研究No.2	JAERI	5022	1968
日本原子力研究所大阪研における放射線化学の基礎研究No.3	JAERI	5026	1969
日本原子力研究所大阪研における放射線化学の基礎研究No.4	JAERI	5027	1970
日本原子力研究所大阪研における放射線化学の基礎研究No.5	JAERI	5028	1971
日本原子力研究所大阪研における放射線化学の基礎研究No.6	JAERI	5029	1972
日本原子力研究所大阪研における放射線化学の基礎研究No.7	JAERI	5030	1973
Annual Report, Osaka Lab., JAERI, No.8	JAERI－M	6260	1974
Annual Report, Osaka Lab., JAERI, No.9	JAERI－M	6702	1975
Annual Report, Osaka Lab., JAERI, No.10	JAERI－M	7355	1976
Annual Report, Osaka Lab., JAERI, No.11	JAERI－M	7949	1977
Annual Report, Osaka Lab., JAERI, No.12	JAERI－M	8569	1978
Annual Report, Osaka Lab., JAERI, No.13	JAERI－M	9214	1979
Annual Report, Osaka Lab., JAERI, No.14	JAERI－M	9856	1980
Annual Report, Osaka Lab., JAERI, No.15	JAERI－M	82－192	1981
Annual Report, Osaka Lab., JAERI, No.16	JAERI－M	83－199	1982
Annual Report, Osaka Lab., JAERI, No.17	JAERI－M	84－239	1983

大阪支所：大阪府寝屋川市三井南町25の1

昭和59度日本原子力研究所大阪支所年報（No.18）
1984年4月1日～1985年3月31日

日本原子力研究所高崎研究所大阪支所

（1986年2月13日受理）

本報告は，大阪支所において昭和59年度に行なわれた研究活動を述べたものである。主な研究題目は，電子及びイオン照射下の界面現象に関する基礎研究，電子線照射による重合反応の研究，ポリマーの改質及び上記の研究と関連して重合反応、高分子の分解及び架橋ならびにグラフト重合に関する基礎的研究などである。

日本放射線高分子研究協会年報	Vol. 1		1958／1959
日本放射線高分子研究協会年報	Vol. 2		1960
日本放射線高分子研究協会年報	Vol. 3		1961
日本放射線高分子研究協会年報	Vol. 4		1962
日本放射線高分子研究協会年報	Vol. 5		1963
日本放射線高分子研究協会年報	Vol. 6		1964
日本放射線高分子研究協会年報	Vol. 7		1965
日本放射線高分子研究協会年報	Vol. 8		1966
日本原子力研究所大阪研における放射線化学の基礎研究No.1	JAERI	5018	1967
日本原子力研究所大阪研における放射線化学の基礎研究No.2	JAERI	5022	1968
日本原子力研究所大阪研における放射線化学の基礎研究No.3	JAERI	5026	1969
日本原子力研究所大阪研における放射線化学の基礎研究No.4	JAERI	5027	1970
日本原子力研究所大阪研における放射線化学の基礎研究No.5	JAERI	5028	1971
日本原子力研究所大阪研における放射線化学の基礎研究No.6	JAERI	5029	1972
日本原子力研究所大阪研における放射線化学の基礎研究No.7	JAERI	5030	1973
Annual Report, Osaka Lab., JAERI, No.8	JAERI－M	6260	1974
Annual Report, Osaka Lab., JAERI, No.9	JAERI－M	6702	1975
Annual Report, Osaka Lab., JAERI, No.10	JAERI－M	7355	1976
Annual Report, Osaka Lab., JAERI, No.11	JAERI－M	7949	1977
Annual Report, Osaka Lab., JAERI, No.12	JAERI－M	8569	1978
Annual Report, Osaka Lab., JAERI, No.13	JAERI－M	9214	1979
Annual Report, Osaka Lab., JAERI, No.14	JAERI－M	9856	1980
Annual Report, Osaka Lab., JAERI, No.15	JAERI－M	82－192	1981
Annual Report, Osaka Lab., JAERI, No.16	JAERI－M	83－199	1982
Annual Report, Osaka Lab., JAERI, No.17	JAERI－M	84－239	1983

大阪支所：大阪府寝屋川市三井南町25の1

CONTENTS

I. INTRODUCTION

Osaka Laboratory was founded in 1958 as a laboratory of the Japanese Association for Radiation Research on Polymers (JARRP), which was organized and sponsored by some fifty companies interested in radiation chemistry of polymers. The JARRP was merged with Japan Atomic Energy Research Institute (JAERI) on June 1, 1967, and the laboratory has been operated as Osaka Laboratory for Radiation Chemistry, Takasaki Radiation Chemistry Establishment, JAERI. The research activities of Osaka Laboratory have been oriented towards the fundamental research on applied radiation chemistry.

The studies on radiation effects on surface phenomena such as adsorption and desorption of gases on the surface of insulating material are important since they will lead to improved understanding of the phenomena occurred on the first wall surface of present-day and future nuclear fusion reactors.

Studies have been carried out in an attempt to clarify the relation between structural change of insulator surfaces and adsorption of gases during electron impact. Single crystal of alumina was bombarded with electrons in vacuo, CO_2, O_2, H_2O or CO while the surface composition was monitored by Auger electron spectrum. CO_2, O_2 and H_2O were found to retard the surface reduction of alumina which proceeds in vacuo. On the other hand, CO showed no such inhibition effect at all and reacted with Al metal on the surface to produce aluminium carbide. The resultant surface containing aluminium carbide no longer sustained surface reduction when electron impact was continued further.

A preliminary study to prepare chemically active or inactive surface by electron beam recoil doping on solid surfaces has been carried out on silicon, silica gel or polyimide surface and iron as injecting element. No definite conclusion has yet been obtained from the change in Auger spectrum during argon ion sputtering in these systems but, it

was found that Kapton surface showed catalytic activity to Fischer-Tropsch reaction, when the polyimide surface had been irradiated with 800 keV electrons in the atmosphere of Ar-iron pentacarbonyl mixture.

Studies were carried out using a glow discharge plasma reactor for ethane, ethylene, acetylene, styrene and other compounds to obtain thin polymer film on aluminium evaporated glass plates. The type of products, film or powder, depends on RF power and pressure of gases, and the reaction conditions to give thin polymer film were systematically surveyed.

Grafting of acrylic acid onto polyester mono filaments was carried out in order to improve the mechanical properties of polyvinylchloride sheet reinforced with polyester fibers, and adhesive strength at interface between polyester filament and polyvinylchloride was found to be improved by the grafting.

The structure of nylon 66 film of various history of thermal treatments and electron irradiation has been studied in an attempt to obtain polymer films of different surface structures on which the studies on thin layer grafting are to be carried out. It is our purpose to know how the reaction rate and structure of the grafting layer are affected by the surface structure of the substrate polymer on the assumption that the surface structure be related to bulk structure of the substrate. Nylon 66 films of different crystallinities have been obtained by thermal treatment of the film.

In the study to assign the thermoluminescence centers of polymeric materials for understanding coloration mechanism of film dosimeters, it was found that the thermoluminescence peaks appeared at three different temperature regions in low density polyethylene were affected by the purification procedures of material and by atmosphere in which the film samples were irradiated.

Dr. Motoyoshi Hatada, Director
Osaka Laboratory for Radiation Chemistry
Japan Atomic Energy Research Institute

II. RECENT RESEARCH ACTIVITIES

1. AES Study on the Relation between Surface Structural Change and Gas Adsorption on Alumina under Electron Impact

Silica and alumina undergo surface reduction under electron impact in an ultra-high vacuum (UHV).[1] Simultaneous impact with Ar^+ ions and electrons also induces the reduction of the insulator surfaces, although the extent of the reduction is lower than that by electron impact because of the predominant occurrence of sputtering of the surfaces during the simultaneous impact. Such a structural change would affect electron or ion impact induced gas adsorption at and desorption from various solid surfaces with which we are mainly concerned. The present study was carried out to find the relation between the surface reduction and the adsorption of gases under electron impact on insulator surfaces.

The apparatus used in this study was the same as described already.[1] Alumina was selected here because it was found to be more liable than silica to charge accumulation during electron impact so that AES measurement could be continued long enough to obtain necessary data for analysis. Alumina samples used were single crystals of sapphire (0.5 mmt, Shinko Co.). The surface of alumina was bombarded with Ar^+ ions and electrons simultaneously until C_{KLL} Auger spectrum due to adsorption of residual gases disappeared completely. Auger electron spectrum was recorded during electron impact in a UHV or in an atmosphere of CO_2 (99.99% up, UHP grade, Seitetsu Kagaku), O_2 (zero U, UHP grade, Seitetsu Kagaku), CO (99.95% up, UHP grade, Seitetsu Kagaku) or D_2O (Nakarai Chemicals Co.). The gas pressure was controlled with a variable leak valve in the lower range than 5×10^{-7} Torr.

Figure 1 shows the change of intensity of Auger signals, O_{KLL}, Al(Ox) due to a cross transition between Al and O, and

Al(M) due to Al metal, with time of electron impact on alumina in 1×10^{-7} Torr CO_2. Both O_{KLL} and Al(Ox) signals decrease in intensity in the initial stage and newly appeared Al(M) grows in intensity with time. The intensities of these signals level off after 20 min. These changes in signal intensity agree qualitatively with those previously found by electron impact on alumina in a UHV, showing the occurence of surface reduction of alumina in a CO_2 atmosphere. The extent of decrease or increase in signal intensity, however, is much lower than that

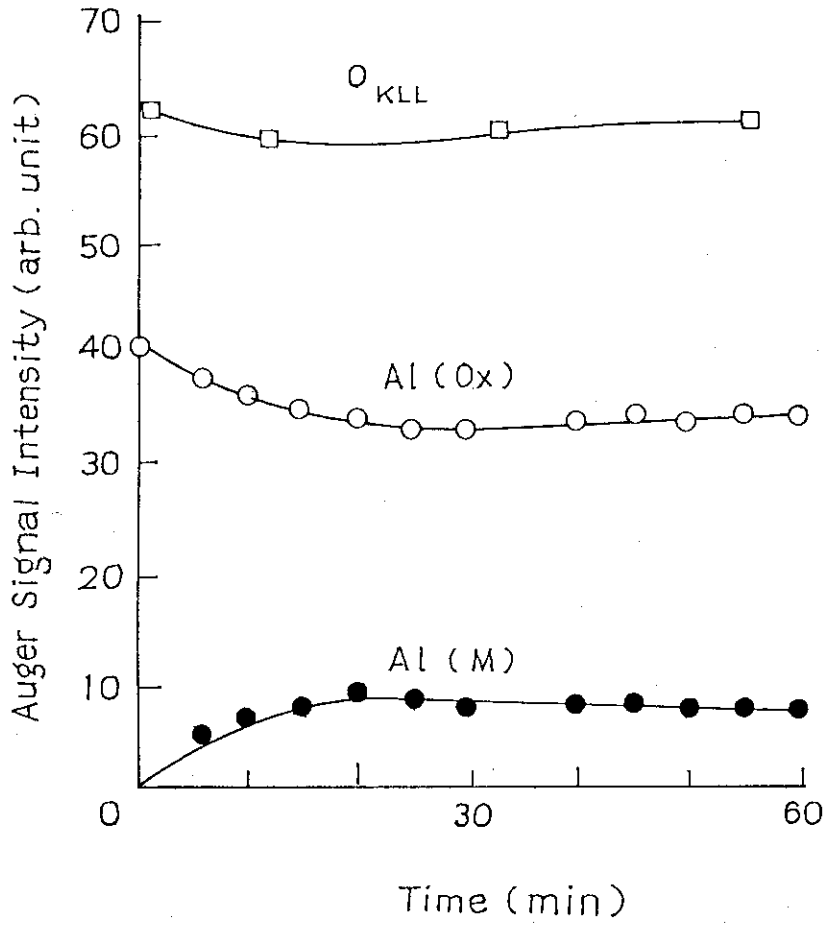

Fig. 1 Variation of Auger signal intensity during electron impact on alumina in 1×10^{-7} Torr CO_2.

in a UHV, which suggests that the surface reduction of alumina is suppressed by CO_2. In fact, no surface reduction was observed during electron impact under CO_2 pressures greater than 5×10^{-7} Torr, as can be seen from Fig. 2 which shows the Auger signal intensity ratio, Al(M)/Al(Ox), in a UHV and under three different CO_2 pressures.

Throughout these experiments, no significant accumulation of carbon on alumina surface was observed in the Auger spectrum. This finding excludes the possibility that CO_2 is adsorbed on alumina either as a parent molecule or as a dissociated molecule containing carbon such as CO irrespective of the presence or absence of Al metal on the surface. The observed effect of CO_2, therefore, may arise from reaction between Al metal on the surface and O atom produced either by dissociative adsorption of CO_2 or by electron induced dissociation of CO_2. In an attempt to learn whether electron beam effect on CO_2 is involved in the formation of O atom or not, alumina was pre-bombarded with electrons in 5×10^{-8} Torr CO_2 while the Auger spectrum was monitored and the resultant surface containing Al metal was brought in contact with 5×10^{-7} Torr CO_2 either in the presence or absence of electron beams. As soon as the surface was exposed to 5×10^{-7} Torr CO_2 in the presence of electron beams, Al(M) disappeared and the intensities of Al(Ox) and O_{KLL} restored to the levels observed before electron impact in 5×10^{-8} Torr CO_2. On the other hand, the exposure in the absence of electron beams resulted in slow decrease of Al(M) intensity and increase of Al(Ox) intensity. This result indicates that the reaction between Al metal and O atom is enhanced by electron beams which can dissociate CO_2 molecule.

Both O_2 and D_2O were found to inhibit the surface reduction of alumina during electron impact as well as CO_2. The results obtained for O_2 agree quantitatively with those for CO_2: The variations of Al(M)/Al(Ox) with impact time in 5×10^{-8} Torr and 1×10^{-7} Torr fit the curves obtained for CO_2

(Fig. 2), and Al(M) did not appear at all in 5×10^{-7} Torr O_2. D_2O showed a stronger effect on the surface reduction than CO_2 and O_2 and no surface reduction took place in 1×10^{-7} Torr D_2O. This finding agrees with the result for oxidation of aluminium which indicates that the oxidation with water vapor is about a factor of 4 faster than with O_2.[2)]

The change of Al(M)/Al(Ox) observed in the early stage of electron impact on alumina in CO atmospheres from 5×10^{-8} Torr to 5×10^{-7} Torr is in accord with that in a UHV, indicating that CO apparently has no effect on the surface reduction of alumina. By prolonged electron impact on alumina in CO atmospheres, however, drastic changes were observed in the Auger spectrum as shown in Fig. 3. C_{KLL}(272) signal appeared, grew in intensity with time and finally levelled off. This

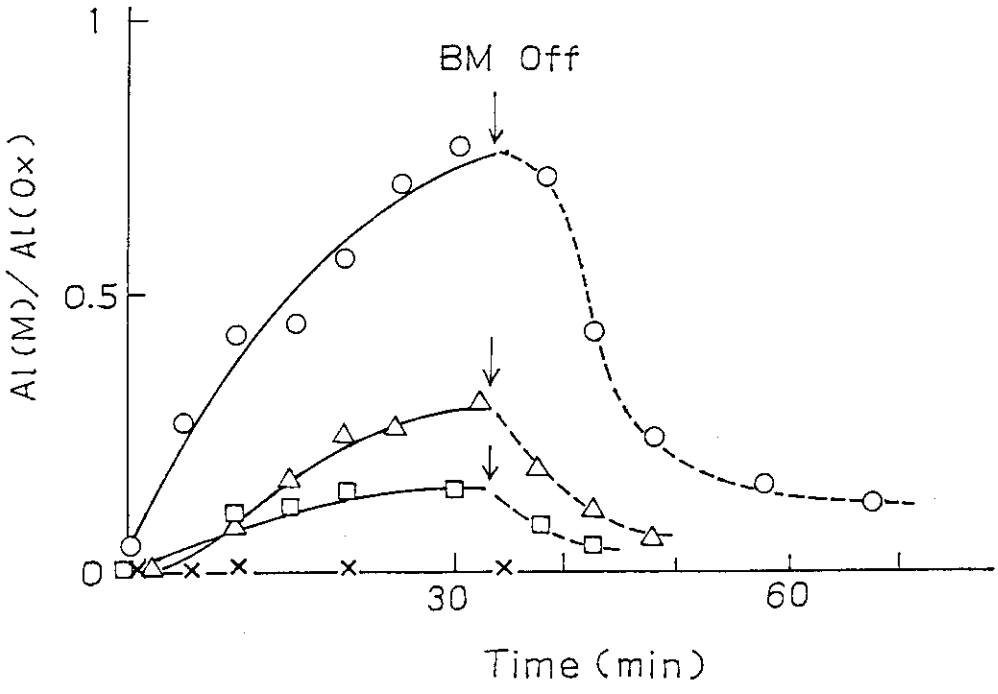

Fig. 2 Variation of Auger signal intensity ratio of Al(M) to Al(Ox) during electron impact of alumina in vacuo (○) and in CO_2 atmospheres at 5×10^{-8} Torr (△), 1×10^{-7} Torr (□) and 5×10^{-7} Torr (×).

C_{KLL} signal is ascribed to carbon in aluminium carbide (Al_4C_3) since the peak energy and signal shape coincide with those reported.[3] O_{KLL}(508) signal gradually decreased in intensity with time. The spectral change in low energy region is shown in Fig. 4 in an expanded scale. The decrease of Al(Ox) in intensity and the appearence of Al(M) and its increase in intensity with time observed in an early stage are the same as observed in a UHV. After 40 min, however, the intensity of Al(M) decreses with time and finally disappeared completely. At the same time, Al(Ox) signal broadens in width and the peak energy shifts from initial 55 eV to final 58 eV. The final peak energy of 58 eV coincides with that for a cross transition $Al_LC_LC_L$, denoted here as Al(C), in Al_4C_3.[3] Therefore, the broad signal with peak energy of 58 eV in Fig. 4f is thought to be an unresolved superposition of Al(Ox) and Al(C).

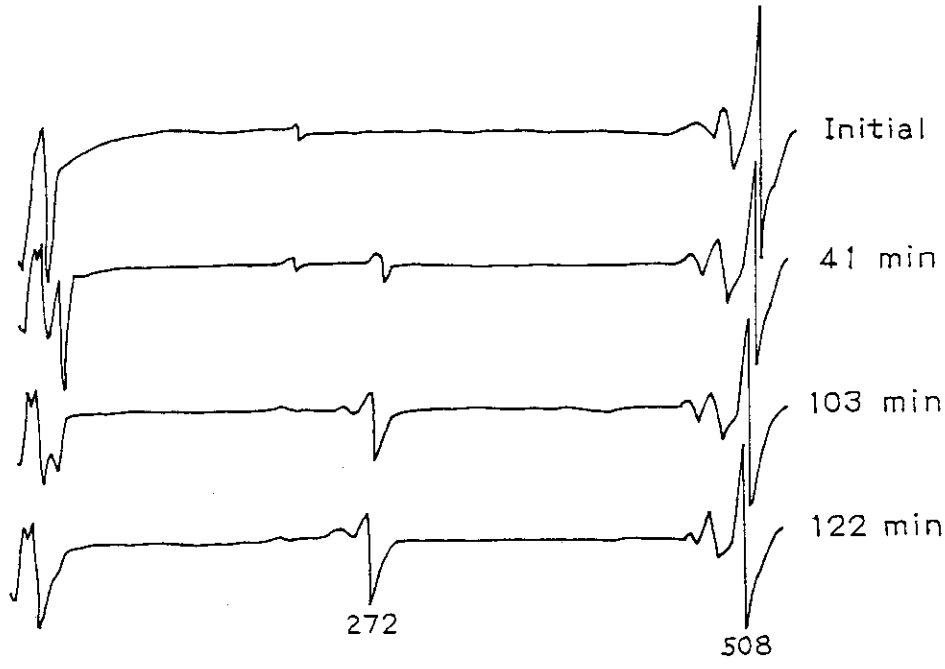

Fig. 3 Change of Auger spectrum of alumina during electron impact in 5 X 10^{-7} Torr CO.

Figure 5 shows the time course of Auger signal intensity of Al(Ox), Al(Ox)+Al(C), Al(M), C_{KLL} and O_{KLL}. The intensity of C_{KLL} increases with time until Al(M) disappears completely. After the disappearence of Al(M), the intensity of C_{KLL} remains constant as well as the intensities of O_{KLL} and [Al(Ox)+Al(C)]. These facts indicate that CO reacts with Al metal on the alumina surface under electron impact to produce Al_4C_3 and that the resultant alumina surface containing Al_4C_3 no longer undergoes surface reduction at all when electron impact was continued further.

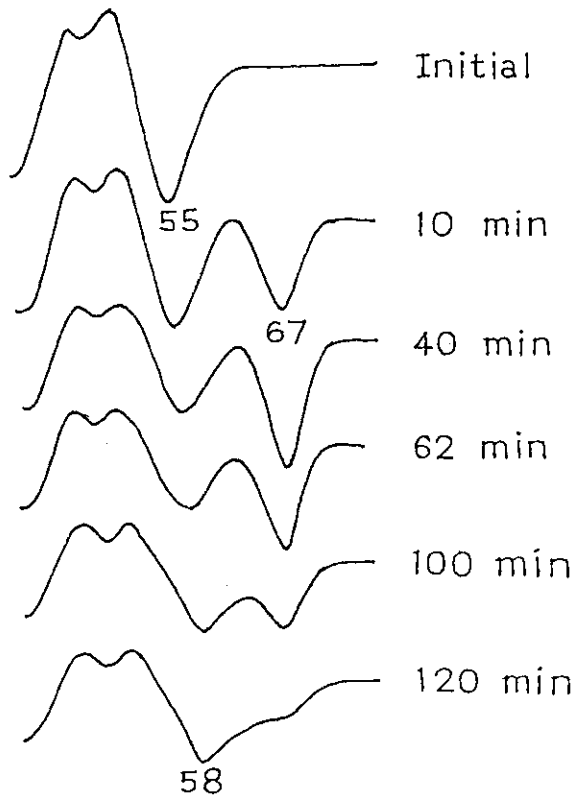

Fig. 4 Change of low energy Auger spectrum(40-75 eV) of alumina during electron impact in 5×10^{-7} Torr CO.

In order to determine whether the species reacting with Al metal to produce Al_4C_3 is CO or C produced from CO by electron impact, an experiment similar to that with CO_2 described above was carried out. The result indicates that the formation of Al_4C_3 occurs only when the alumina surface containing Al metal is exposed to CO in the

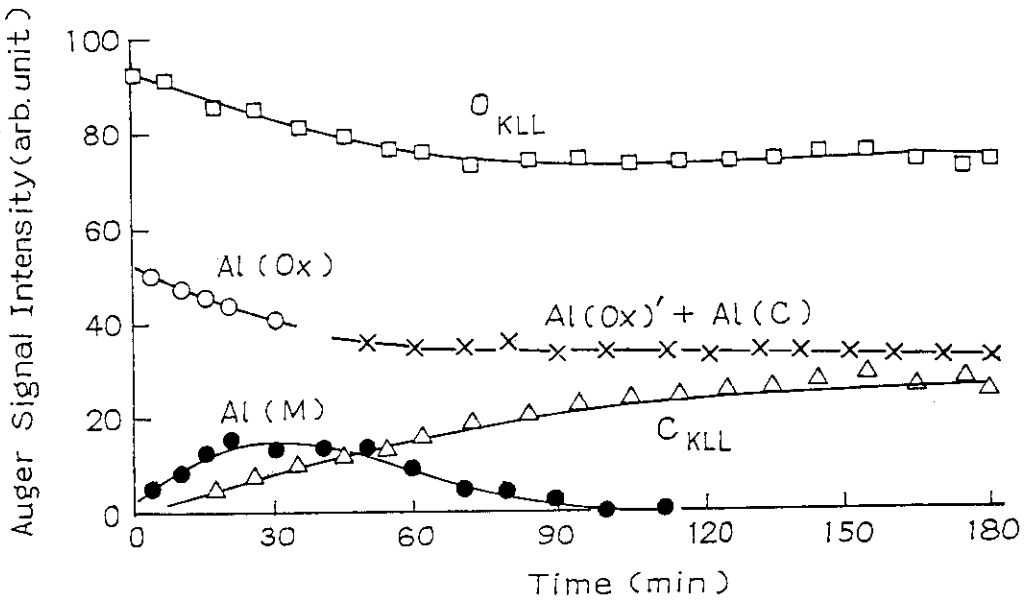

Fig. 5 Variation of Auger signal intensities of Al(Ox), Al(M), O_{KLL} and C_{KLL} during electron impact on alumina in 5×10^{-7} Torr CO. Data marked by X denote the intensity of Al(Ox) + Al(C) .

presence of electron beams. Therefore, it can be concluded that the reaction involving C atoms produced by electron induced dissociation of CO is responsible for the formation of Al_4C_3.

(S. Nagai)

1) S. Nagai and Y. Shimizu, J. Nucl. Mat., 128/129, 605 (1984).
2) W. Eberhardt and C. Kunz, Surf. Sci., 75, 709 (1978).
3) S. A. Flodström and C. W. B. Martinsson, Appl. Surf. Sci., 10, 115 (1982).

2. Structural Changes of SiO_2 and Si Surfaces during Electron Impact

In order to examine adsorption and desorption process of simple inorganic gases at the surface of silica under electron beam impact, the change of the surface structure was monitored by Auger electron spectra recorded during electron impact on SiO_2 in vacuo. For comparison, Auger spectra were recorded during electron impact on n-Si(111) in 5×10^{-7} Torr O_2 and in vacuo after interrupting O_2 supply.

SiO_2 (quartz crystal, Nakarai Chemicals Co.), n type Si(111) (Nihon Silicon Co.) and α type SiC (Nippon Carbon Co.) were obtained in the forms of sheet, wafer and disk from commercial sources. Electron impact and measurement of Auger spectrum were carried out with an AES/SIMS equipment (AES-350S, Nichiden Anelva) described previously.[1] The base pressure during the experiments was typically $\sim 2 \times 10^{-9}$ Torr. Electron beam energies used were 0.6, 0.75, 1.0 and 1.5 keV. Auger spectra were measured using $2V_{pp}$ modulation.

Auger electron spectrum of SiO_2 gives mainly a strong peak at 80 eV due to a Si_{LVV} transition and a peak at 509 eV due to an O_{KLL} transition. The signal intensities of Si(80) and O_{KLL}(509) decrease gradually with electron impact time. On the other hand, a peak at 93 eV due to Si_{LVV} from a pure silicon appears in the first 2 min of electron impact of 1 keV and increases in intensity with time but its intensity reaches constant value after 140 min. These results agree well with those reported already for silica gel[2] and silica glass,[3] and indicate that electron impact on SiO_2 induces scission of Si-O bonds followed by loss of O atoms, resulting in reduction of the surface. Similar results were also obtained by impact with 0.6, 0.75 and 1.5 keV electrons. A prolonged impact (about 40 min) with 1.5 keV electrons resulted in the distortion of the spectrum owing to charging up of the sample. However, no indication of charging up was observed at least for 140 min

with impact with 1.0 keV electrons.

Figs. 1-2 show the plots of the change of the peak heights of $Si_{LVV}(80)$ and $O_{KLL}(509)$ relative to the initial values with time of impact with 1.5, 1.0, 0.75 and 0.6 keV electrons. As can be seen from Fig. 1, the relative peak height of $Si_{LVV}(80)$ agrees with that of $O_{KLL}(509)$ under impact with 1.5 and 1.0 keV electrons. In contrast, they differ from one another under impact of 0.75 and 0.6 keV electrons and the relative peak height of $Si_{LVV}(80)$ is always greater than that of $O_{KLL}(509)$.

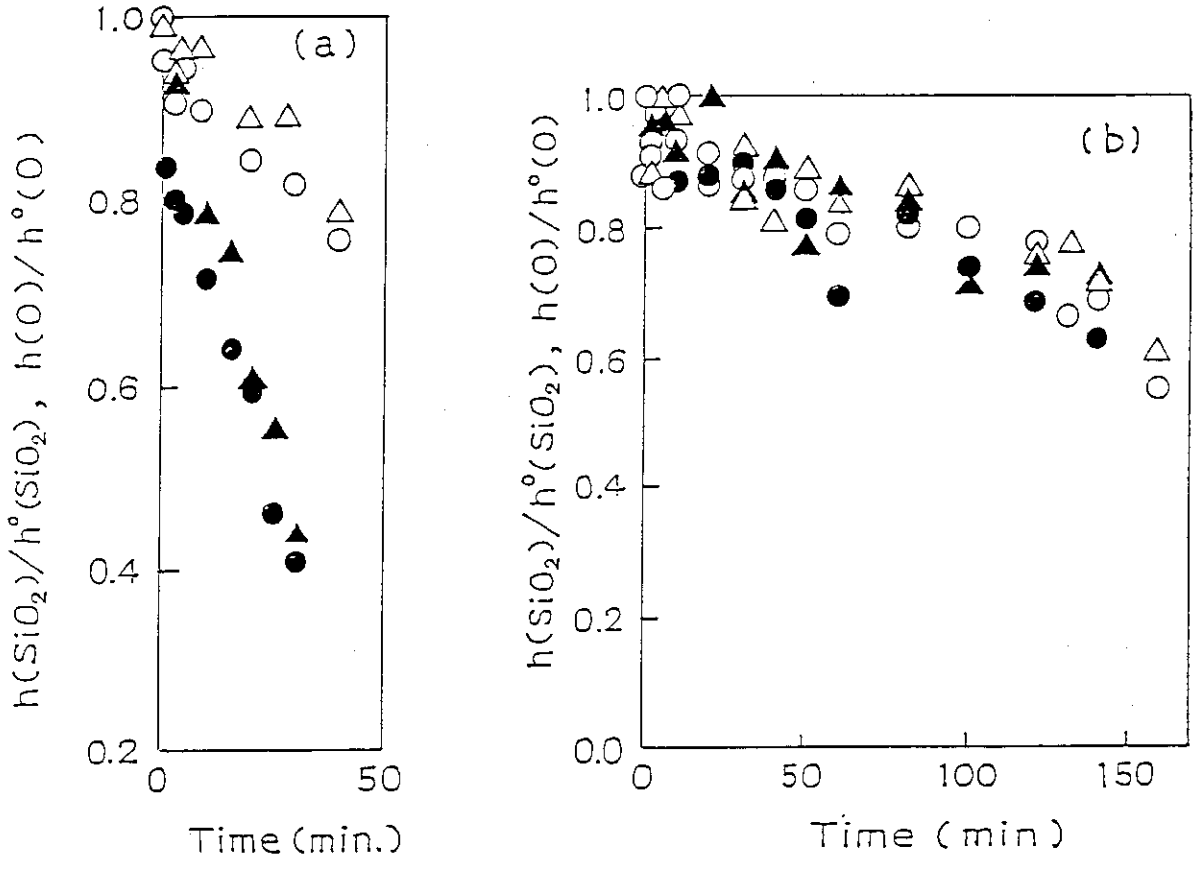

Fig. 1 Plots of $h(SiO_2)/h\ (SiO_2)$(,) and $h(O)/h\ (O)$(,) during impact with 1.5 keV(a) and 1.0 keV(b) electrons on SiO_2. Open, the first run; Closed, the second run.

These findings suggest that the mechanism of reduction of SiO_2 induced by impact with 1.5 and 1.0 keV electrons is different from that induced by impact with 0.75 and 0.6 keV electrons. Lang et al[4] have found from the measurements of Auger spectra during thermal oxidation of Si(111) that an intermediate oxidation stage characterized by the SiO_x ($x \simeq 1$) formation exists in the oxidation process of Si and appears under mild conditions at the early stages of oxidation. They also have reported that it is slightly enhanced by ion- and/or electron-bombardment of SiO_2. Accordingly, it may be considered that the reduction of SiO_2 induced by impact with 0.75 and 0.6 keV electrons proceeds via an intermediate reduction species (SiO) in contrast to the reduction by impact with 1.5 and 1.0 keV electrons.

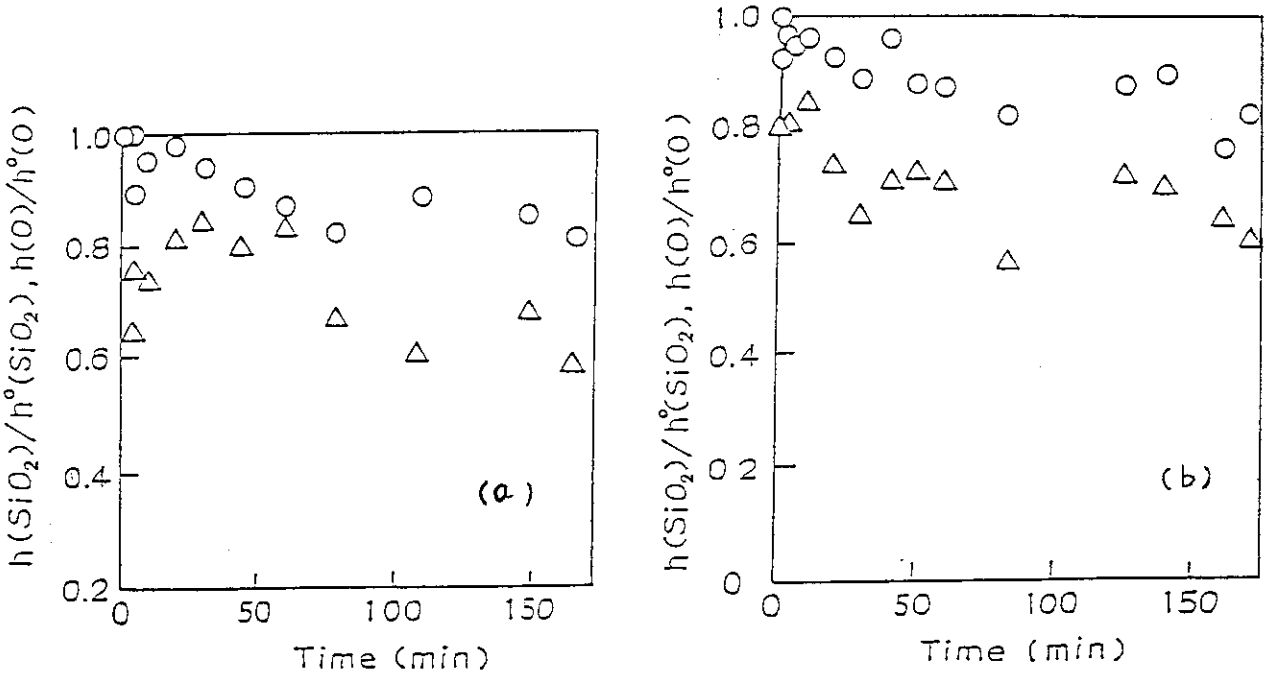

Fig. 2 Plots of $h(SiO_2)/h^0(SiO_2)$(○) and $h(O)/h^0(O)$(△) during impact with 0.75 keV(a) and 0.6 keV(b) electrons on SiO_2.

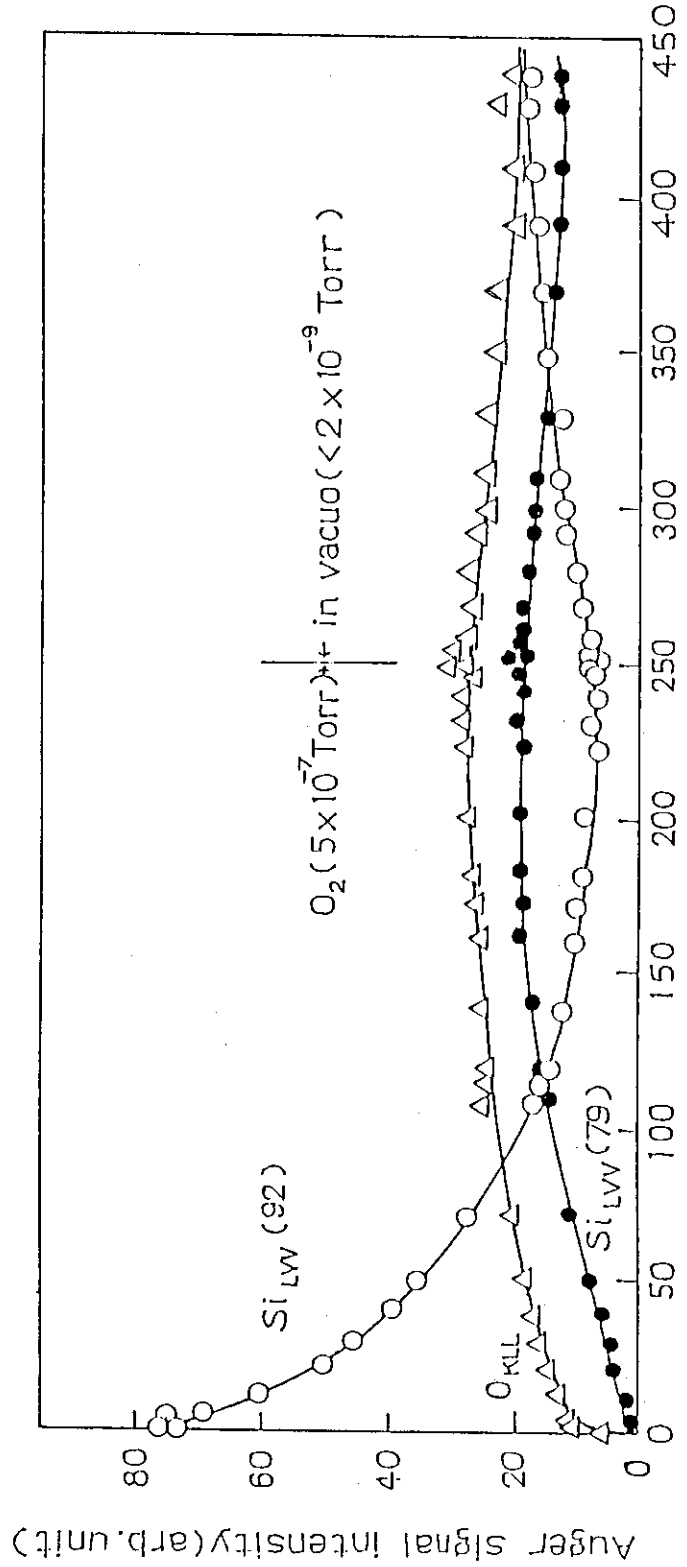

Fig. 3 Variation of Auger signal intensities of n-Si(111) during impact of 1.5 keV electrons in 5 X 10^{-7} Torr O_2 and during electron impact in vacuo.

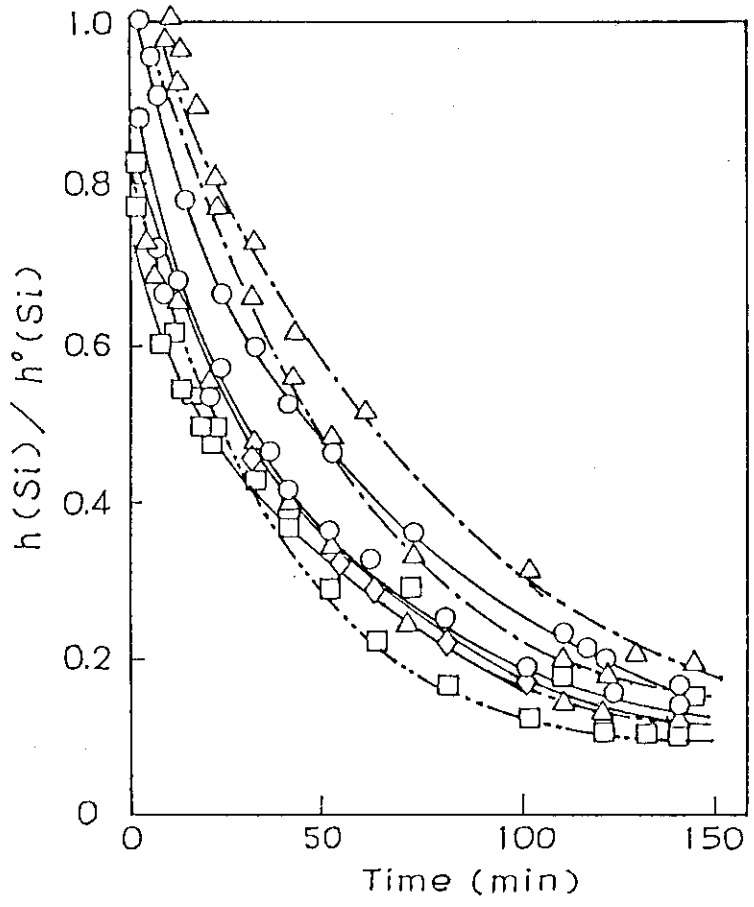

Fig. 4 Plots of $h(Si)/h^{\circ}(Si)$ of n-Si(111) during electron impact with (○), 1.5; (△), 1.0; (□), 0.75 and (◇), 0.6 keV in 5×10^{-2} Torr O_2.

Fig. 3 shows the variation of Auger signal intensities of n-Si(111) during impact with 1.5 keV electrons in 5×10^{-7} Torr O_2 and in vacuo after interrupting O_2 supply. Auger electron spectrum of clean n-Si(111) gives a peak at 93 eV due to a Si_{LVV} transition. The signal intensity of $Si_{LVV}(93)$ decreases rapidly with increasing impact time and new peaks appear at 75 eV due to a Si_{LVV} transition[2] and 509 eV due to an O_{KLL} transition in the O_2 atmosphere. The peak energy of 75 eV soon shifts to a value of 80 eV. The peaks of $Si_{LVV}(80)$ and $O_{KLL}(509)$ increase gradually in intensity. However, signal intensities of these three peaks all reach constant values after 250 min in O_2. These results indicate that electron impact of n-Si(111) in an O_2 atmosphere results in oxidation of the surface.[5] Similar results were also obtained by impact with 0.6, 0.75 and 1.0 keV electrons. Fig. 4 shows the change of relative peak height of $Si_{LVV}(93)$ with time of electron impact in 5×10^{-7} Torr O_2. It can be seen from Fig. 4 that the rate of oxidation of n-Si(111) is almost independent of energy of incident electrons in the range of $0.6 \sim 1.5$ keV. When these oxidized n-Si(111) samples were bombarded with electrons in vacuo, the reduction reaction of the surface proceeds very slowly but does not recover to the levels observed before oxidation, as shown in Fig. 3.

(Y. Shimizu and S. Nagai)

1) S. Nagai, and Y. Shimizu, JAERI-M 83-199, 40 (1983).
2) S. Thomas, J. Appl. Phys., 45, 161 (1974).
3) S. Nagai, and Y. Shimizu, J. Nucl. Mater., 128/129, 605 (1984).
4) B. Lang, P. Scholler and B. Carriere, Surf. Sci., 99, 103 (1980).
5) For example, B. Carrière and J. P. Deville, Surf. Sci., 80, 278 (1979).

3. Electron-Beam Recoil Doping of Iron to Kapton

It was reported that atoms can be injected into substrate by electron-beam recoil doping method.[1] Studies were carried out in an attempt to know whether chemical modification of the silicon surface can be achieved by doping iron from penta-carbonyl iron vapor by this method, but no definite conclusion was yet obtained so far. This year, we selected polyimide (Kapton 500 H, 125 μm in thickness), as the surface and iron as the material to be injected to give catalytic activity for Fischer-Tropsch reaction to the surface.

Electron irradiation of the samples was carried out using an electron accelerator of rectifying transformer type at the accelerating voltage of 800 kV and beam current of 2 mA for 7200 sec under an argon stream (flow rate: 36ℓm /min) containing iron pentacarbonyl in a flow type reaction vessel (FIXCAT-II) made of stainless steel with titanium irradiation window on top.

After irradiation with electron beam, the Kapton film was immersed in 0.1 N HCℓ aq. solution to remove deposited iron on the surface and then subjected to surface analysis using a SIMS-Auger System (AES-350 S) to observe the change of Auger electron spectrum during Ar^+ sputtering which was carried out at accelerating voltage of 5 kV and source pressure of 4.0 div.

Catalytic activity of the solid surface to Fischer-Tropsch reaction was examined using a gas flow recycling system composed of a reaction vessel (10 mm in diameter, and 200 mm long), a gas reservoir (1.1 ℓ in capacity), and a gas sampler which automatically injects 1 mℓ reacting gas from the circulating flow system into a gaschromatograph at a constant repetition period. The reactant gas was a mixture of 1 : 4 by volume of CO and H_2 at 1×10^5 Pa and the temperature of catalysts was from 250 to 300°C.

Auger study on depth profile has not been very reliable depending on the examination spot on the surface. Figure 1

shows an example of a depth profile of Kapton film. The Auger peaks due to Cℓ(KLL) and O(KLL) decreased with sputtering time, whereas Auger peaks due to Fe(LMM) increased with increasing sputtering time. The results seem to indicate that Cℓ and O are present on the surface and Fe is implanted in some concentration below the surface.

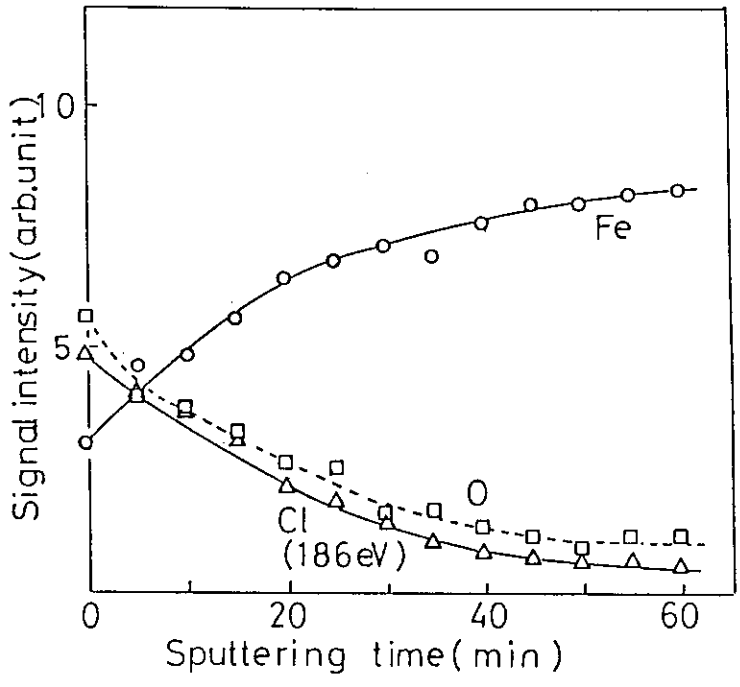

Fig. 1 Intensities of Auger peaks as a function of sputtering time.

Figure 2 shows the amounts of Fischer-Tropsch reaction products as a function of time. The reaction temperature was increased stepwise from 255°C to 304°C. The amounts of products were given in μ mole and normalized to the amount per 10 cm^2 surface area of Kapton and per 1 ℓ reactant. The amounts of products linearly increased in the isothermic region and the slopes increased as the reaction temperature increased except at later stage of the reaction at 304°C where catalytic activity decreased.

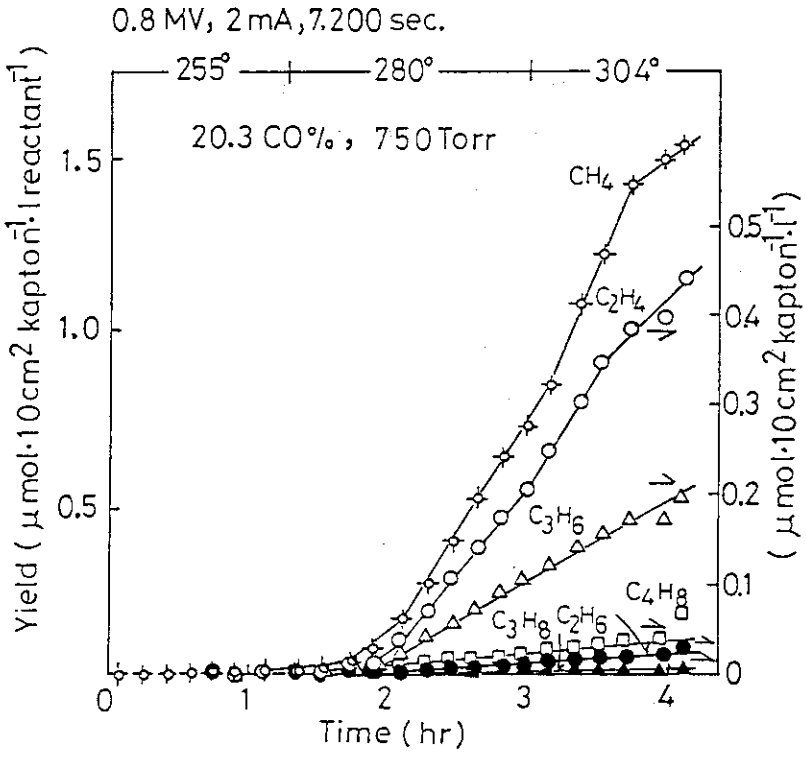

Fig. 2 The yiels of the products as a function of reaction time; 0.8 MV, 2 mA, 7,200 sec.

The Arrhenius plots of CH_4 and C_2H_4 in Fig. 3 give activation energies of 13.8 and 7.4 kcal/mole, respectively, which are within the range of activation energies reported in the literature.[2)]

The catalytic activity as given by the rate of product formation is plotted as a function of electron accelerating voltage employed in recoil doping in Fig. 4, where the catalytic activity slightly observed at 500 kV and increased linearly with increasing the voltage.

In Fig. 5 the catalytic activity is plotted as a function of electron doping time. The activity producing CH_4 increased with increasing doping time almost linearly, but the activities producing higher hydrocarbons increased only a little for early period of doping and then increased linearly with increasing

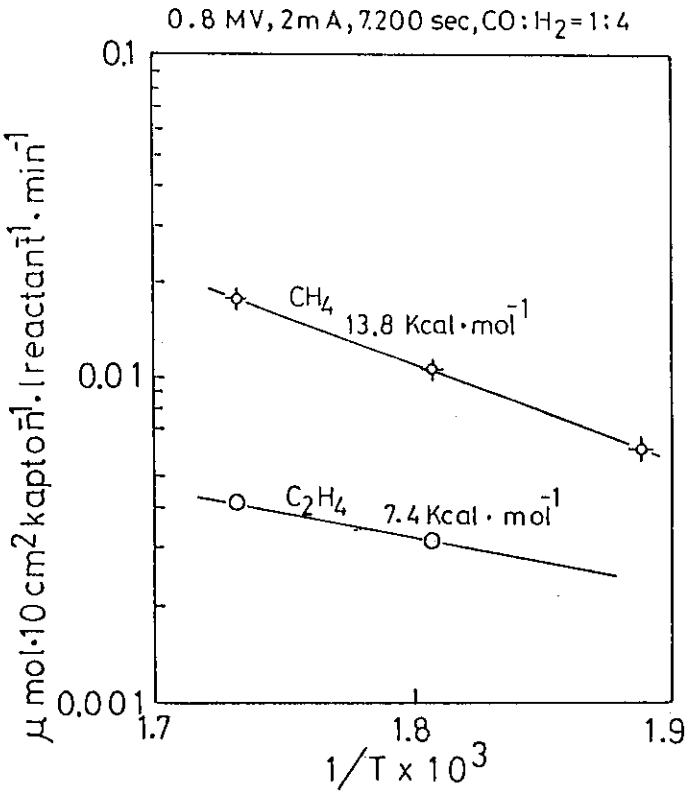

Fig. 3 Arrhenius plot; 0.8 MV, 2 mA, 7.200 sec. CO : H_2 = 1 : 4

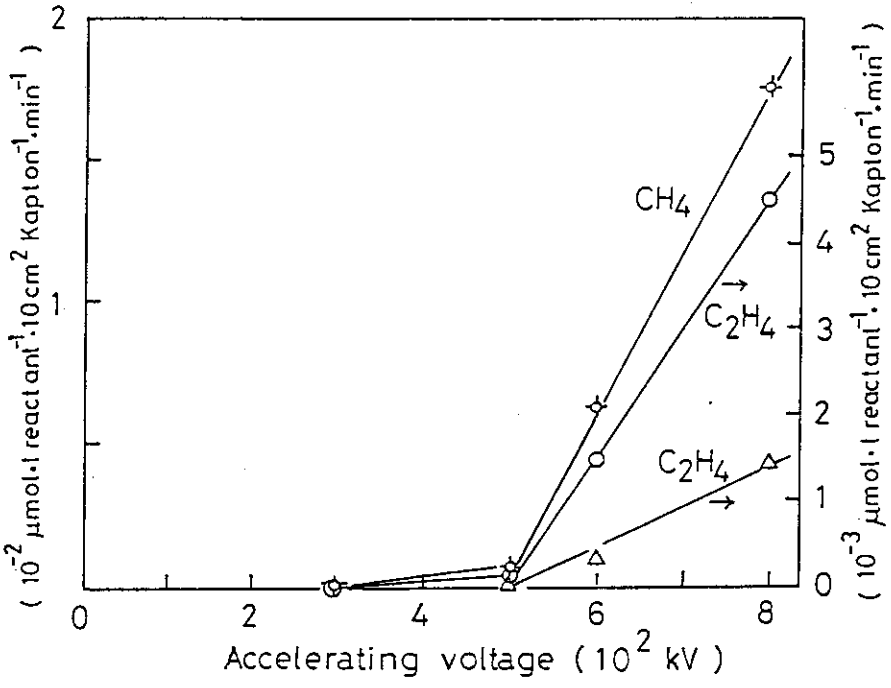

Fig. 4 Catalytic activity as a function of electron accelerating voltage.

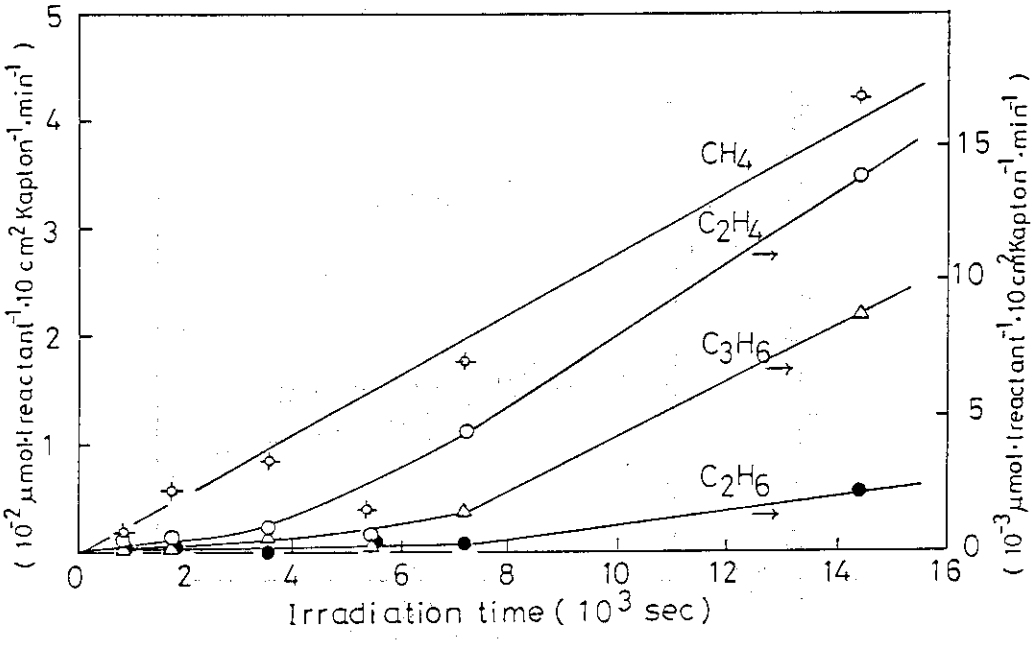

Fig. 5 Catalytic activity as a function of irradiation time.

doping time. This period of irradiation giving little activity to the surface seems to be longer for the activities producing higher hydrocarbons. The reason for this is not clear at present, but it seems that the activities for higher hydrocarbons are higher for the larger size of clusters of iron atoms which becomes abundant when irradiation continues longer.

Similar doping experiment carried out for Kaptone film upon which iron had been deposited by vacuum evaporation method did not show any activity to Fischer-Tropsch reaction. This indicates that the energy obtained by iron atoms by electron recoil process may be less than a certain threshold value which is necessary to release iron atoms from the crystal lattice of iron layer deposited on Kapton surface.

(S. Sugimoto and M. Hatada)

1) T. Wada, et al., Proc. 6th Symp. Ion Source and Ion Assisted Tech., (Tokyo),432 (1982).
2) D. J. Dwyer and G. A. Somorjai, J. Catal.,52, 291 (1978).

4. Thermoluminescence Spectra of Irradiated Low Density Polyethylene

Studies have been carried out in an attempt to elucidate the mechanism of thermoluminescence observed in irradiated low density polyethylene.

The glow curves and spectra of the thermoluminescence were measured on polyethylene[1] purified by precipitation from hot xylene solution, polyethylene containing additives and commercially available polyethylene without further purification (Sumikathene). The glow curves were obtained using the apparatus described in the previous report.[2]

The spectra of the luminescence were measured using the same apparatus with a monochrometer inserted in its optical path as shown in Fig. 1. The peak appeared at 110 K in the glow curve obtained by 20 kGy irradiation was not observed under vacuum below 10^{-3} Pa, but observed in air or a He atmosphere (10^{5} Pa). The same behavior of the peak was also observed for polyethylene containing additives.

Fig. 2 shows the glow curves obtained for Sumikathene in the presence of He at 10^{5} Pa at different doses. Three peaks are recognized at 110 K, 180 K and 250 K in the glow curve at 0.2 kGy.

It can be inferred that the low temperature peak (appeared at 110 K) and high temperature peak (250 K) are related to the temperatures at which the rotational motion of the terminal groups (γ-transition) and the molecular motion of the main chain (β-transition) begin, respectively, from the change of trapped radical concentration as a function of increasing

temperature.[3)]

No information on the origin of the glow peak observed at 180 K was obtained because the intensity of this peak and temperature of the peak maximum depend on the experimental conditions such as the concentration of additives. As shown in the figure, the intensity of the low temperature peak (110 K) increased with increasing dose up to 400 kGy, and then seemed to be leveled off above this dose. On the other hand, the intensity of the high temperature peak (250 K), which is supposedly originated from polyethylene itself, increased with increasing dose up to 20 kGy and then decreased sharply with increasing dose and the peak disappeared at 400 kGy. Dose dependence of the intensity of the peak at 180 K, which possibly arises from the impurity, was not reproducible.

In Fig. 3, the glow curves observed at 10^{-3} Pa are shown for the samples irradiated at different doses. The low

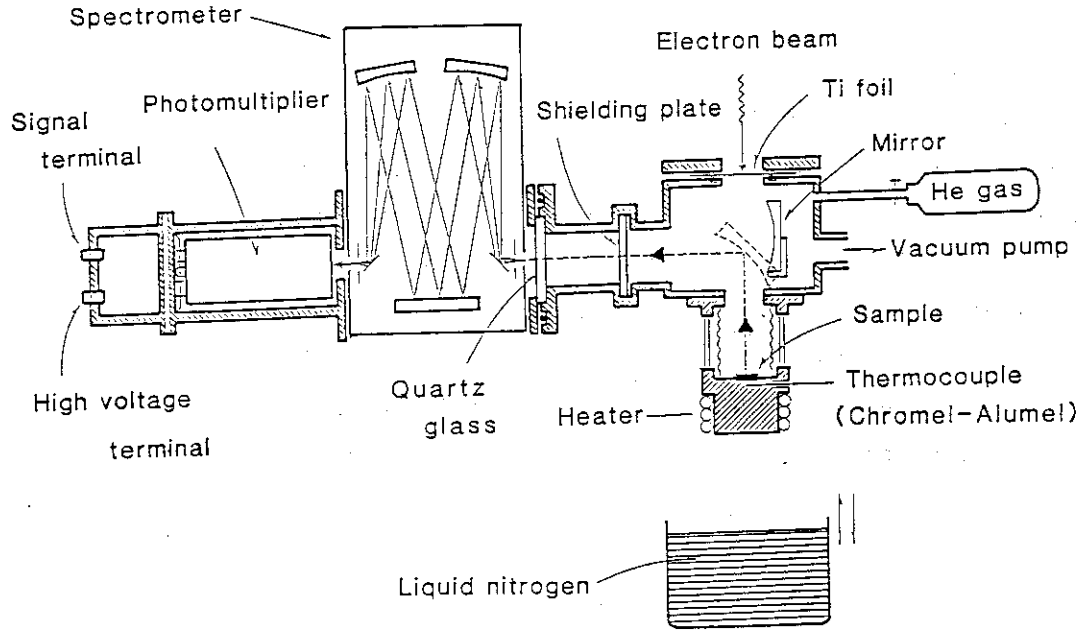

Fig. 1 Experimental apparatus for thermoluminescence measurement.

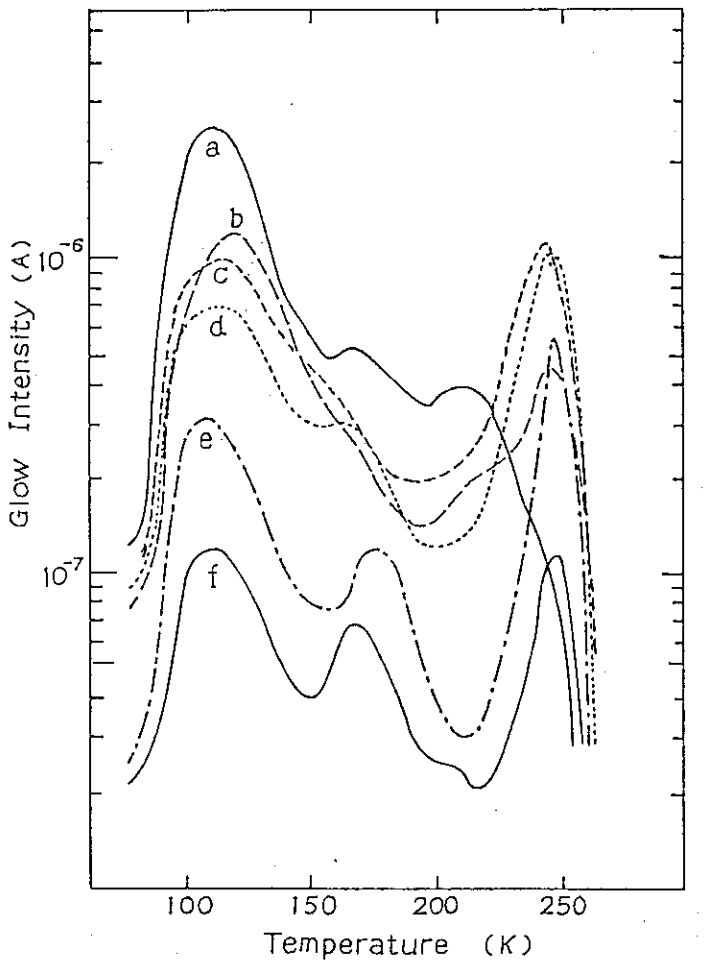

Fig. 2 Thermoluminescence glow curves for LDPE (Sumikathene) in a He atmosphere (10^5 Pa).
a: 400 kGy, b: 40 kGy, c: 20 kGy,
d: 10 kGy, e: 1 kGy, f: 0.2 kGy.

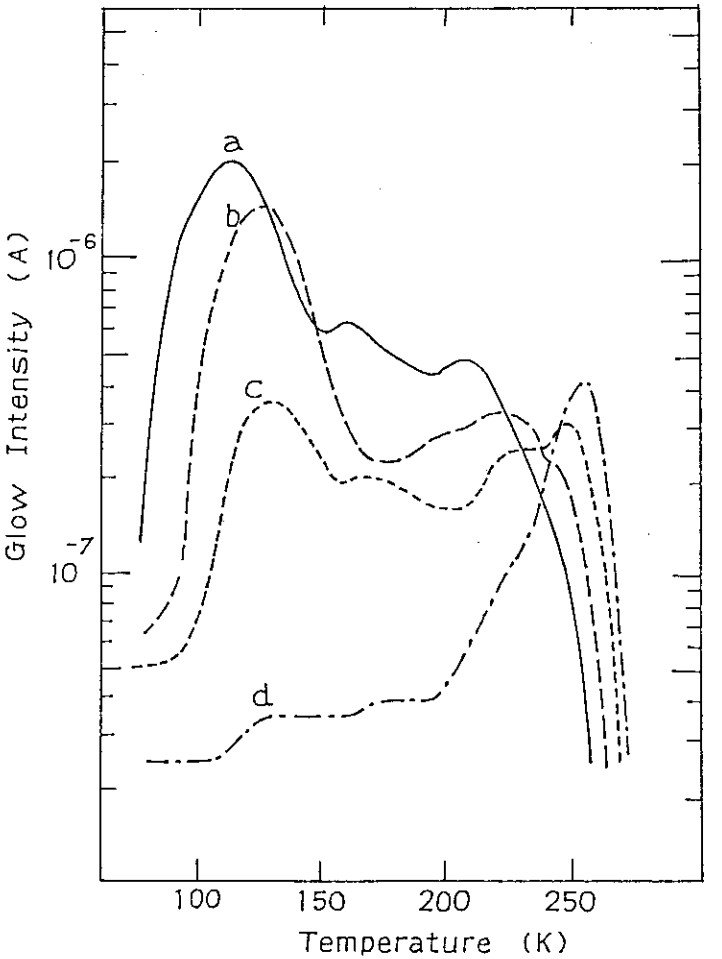

Fig. 3 Dose dependence of thermoluminescence glow curves for LDPE (Sumikathene) in vacuo (10^{-3} Pa).
a: 400 kGy, b: 100 kGy, c: 40 kGy,
d: 20 kGy.

temperature peak was not observed for the samples irradiated below 20 kGy but clearly observed at doses above 40 kGy. In order to know whether this phenomenon was occurred due to gas occluded in the samples, the samples were heat-treated in vacuo (at 10^{-3} Pa) at 393 K for 30 min and 433 K for 30 min before irradiation to remove gas which may be occluded in the sample.

As shown in Fig. 4 the low temperature peak did not appear in the glow curve obtained for the sample pre-heat treated at 393 K and then irradiated at 40 kGy as expected, but appeared in the glow curve for the sample pre-heat treated at 433 K and then irradiated at the same dose. The reason that the low temperature peak was observed for the latter sample is probably because the gas evolved from polyethylene by thermal decomposition results in the optical emission.

In order to study what species are responsible for the luminescence, optical emission spectra were measured. The spectra were measured at temperatures every 10 K while the temperature of the sample increased at heating rate of 10 K/min from 77 K. The wave length range of the measurement was 200-600 nm and time necessary for scanning this range was about 20 sec. In Fig. 5 the thermoluminescence spectra obtained for Sumikathene irradiated at 20 kGy in a He atmosphere (10^5 Pa). The numerals at left indicate the temperature when the wave length scanning begins at 200 nm. Two peaks appeared at 310 nm and 430 nm in the spectrum of the low temperature peak, a weak and broad peak at 500 nm in the spectrum of the intermediate temperature peak, and a sharp and strong peak at 340 nm and a weak peak at 510 nm in the spectrum of the high temperature glow peak. The wave lengths at which the peak maximum appears were the same for the samples of different qualities, such as those containing no impurity, or containing one like antioxidant such as methyl phenol, as long as the dose given to the samples was 20 kGy. Also, no wave length shift of the peaks was observed by the presence of any types of gases. This finding suggests that the luminescence may not directly

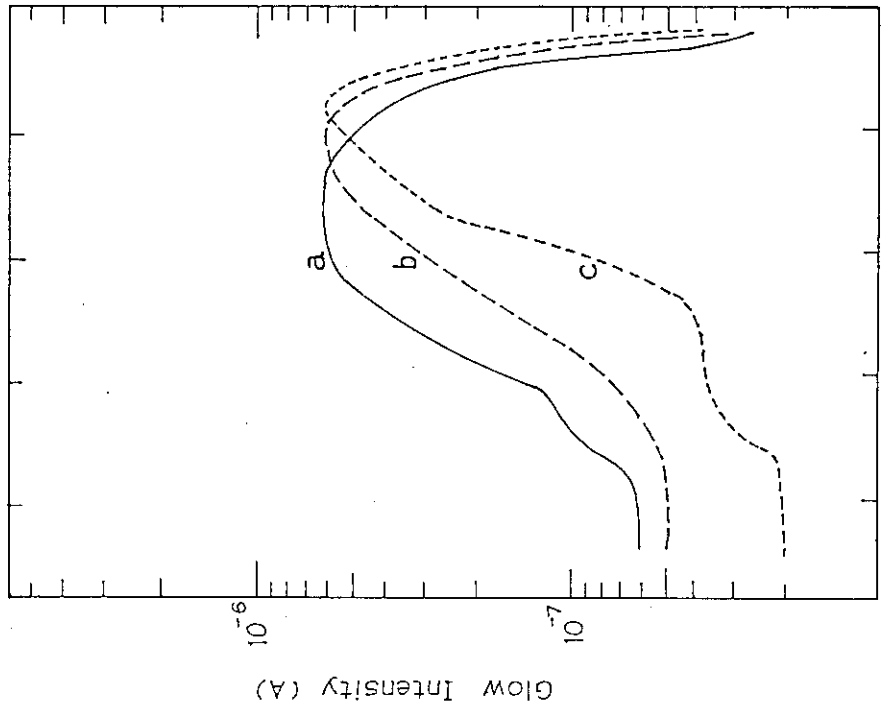

Fig. 4 Thermoluminescence glow curves for LDPE (Sumikathene) in vacuo (10^{-3} Pa) pre-heat treated at 393 K for 30 min.
a: 1200 kGy, b: 200 kGy, c: 40 kGy.

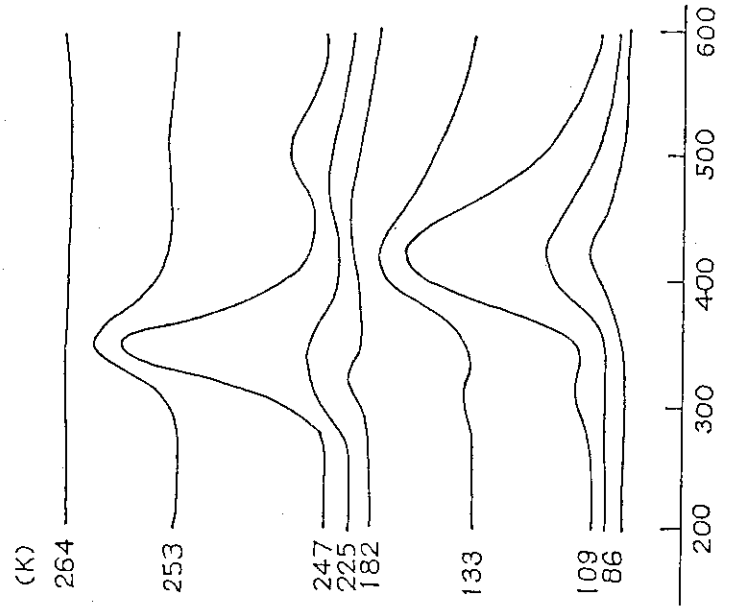

Fig. 5 Thermoluminescence spectra for LDPE (Sumikathene) irradiated at 20 kGy in a He atmosphere (10^{5} Pa).
The numerals at left indicate the temperature when the wave length scanning begins at 200 nm.

come from the impurity or ambient gas, but from polyethylene itself.

The low temperature peak was not observed in the glow curve obtained for the sample irradiated in vacuo at 20 kGy, but was observed when the sample had been irradiated in vacuo at 40 kGy in advance. The luminescence spectra measured on the low temperature peak for the sample irradiated in vacuo at 40 kGy was the same as that measured on the low temperature peak in other conditions, as shown in Fig. 6, and therefore, the origin of the low temperature peak is the same for these samples. A possible origin of the low temperature peak may be CH^* (A-X band, 431 nm) produced from polyethylene by discharge

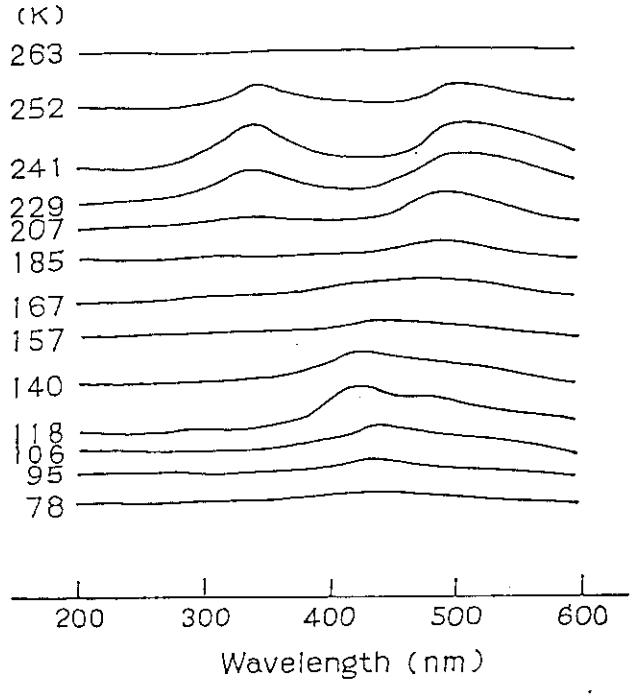

Fig. 6 Thermoluminescence spectra for LDPE (Sumikathene) irradiated at 40 kGy in vacuo(10^{-3} Pa). The numerals at left indicate the the temperature when the wave length scanning begins at 200 nm.

of electrons released from the trap sites in the matrix. The small peak at 300 nm in the luminescence spectra of the low temperature peak is possibly assigned to the CH^* (C-X band, 314 nm).

The change of the luminescence spectra with increasing dose is shown in Fig. 7, where it is evident that the two peaks at 310 nm and 430 nm which are observed in the low temperature peak decreased with increasing dose and almost disappeared at 400 kGy, on the other hand, the peak at 510 nm appeared at 40 kGy and its intensity increased with dose.

The two peaks at 340 nm and 510 nm were observed in the spectra of the high temperature peak (250 K) which is observed in the glow curve of the sample irradiated at 20 kGy. The peak

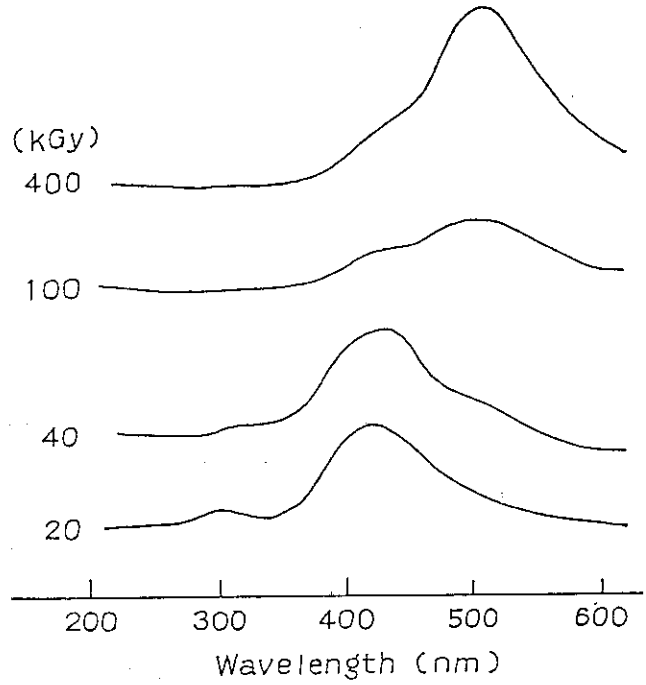

Fig. 7 The change of the luminescence spectra with increasing dose in the low temperature peak(110 K). Sample: Sumikathene.

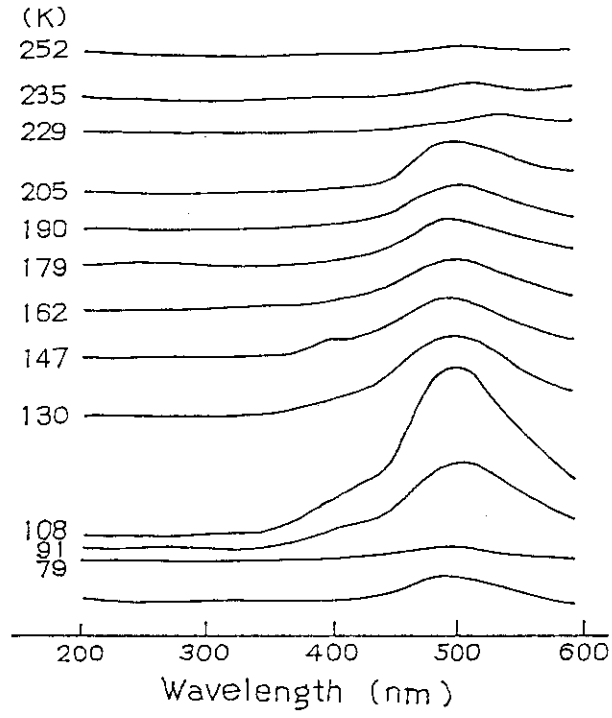

Fig. 8 Thermoluminescence spectra for LDPE (Sumikathene) irradiated at 400 kGy in vacuo (10^{-3} Pa). The numerals at left indicate the temperature when the wave length scanning begins at 200 nm.

at 340 nm decreased with dose and the peak at 510 nm alone was still observed at 400 kGy. An example of this phenomenon is shown in Fig. 8 which shows the luminescence spectrum from Sumikathene irradiated in vacuo at 400 kGy. This phenomenon was observed irrespective of purity of the sample or the presence of the ambient gas. The strong band at 510 nm is tentatively assigned to C_2^* swan band ($A^3\pi_g \rightarrow X^3\pi_u$) emission from fragments of polymer chain, which may exist favorably at large dose.

(K. Matsuda and Y. Tsuji)

1) K. Matsuda, Y. Nakase, Y. Kumakiri and Y. Tsuji, JAERI-M 85-044 (1985).
2) K. Matsuda, Y. Nakase, Y. Tsuji and I. Kuriyama, JAERI-M 84-239, 29 (1985).
3) H. Kashiwabara, Japan. J. Appl. Phys., 3, 384 (1964).

5. Preparation of Thin Polymer Film by Plasma Reaction of Ethane, Ethylene and Acetylene

Studies have been initiated on the plasma polymerization of hydrocarbons to obtain thin polymer film comparatively with electron beam polymerization of acetylene in an attempt to seek the reaction condition resulting in thin polymer films in the electron beam polymerization. It is reported that cuprene is produced instead of polymers in a film form when acetylene is exposed to ionizing radiation.[1,2] Plasma polymerization, on the other hand, produces polymers of thin film type,[3,4] but the film is highly crosslinked and is of electrically insulating property. It is interesting to study the feature of radiation and plasma chemical reactions and to know the properties of the products thus obtained.

Acetylene was obtained from Kanto Acetylene Industries, Co. and used as received or after removal of acetone by bubbling through sodium bisulphate aqueous solution followed by drying over calcium oxide. Ethane and ethylene were of "research" grade and were obtained from Takachiho Chemicals Co. and used without further purification. Benzene and styrene were of reagent grade supplied by Nakarai Chemicals Co. Acetylene was stored in a 10 liter glass bulb after repeated cycles of freezing and evacuation to remove air which was sneaked in the gas during transfer from a gas tank to the gas reservoir. The irradiation vessel was connected with a glass connecting tube equipped with ball joints (J. Young and Co. 28/15) at both ends, and then the vessel was evacuated to

10^{-3} Torr.

Gases were introduced into the vessel to a desired pressure which is measured by a semiconductor pressure gauge (Toyota Koki Type PMS-5-2H). Electron beam irradiations were carried out in a vessel made of stainless steel (SUS 304) which had been used for radiation chemistry of CO-H_2 gas.[5] The vessel is of 7.1 liter in volume and is equipped with (a) aluminium irradiation window (0.1 mm in thickness) at top, through which electron beam penetrates,(b) pressure sensor used for measuring gas pressure during irradiation, (c) pressure sensor to glass plates set at a definite position on which products are accumulated, (d) film thickness gauge and (e) a teflon stopcock (Ace glass) and greaseless ball joints (28/15) through which the reactant is introduced for irradiation or the gas is pumped off for analysis after irradiation.

During irradiation, the pressure change was followed by the pressure gauge.

After electron beam irradiation, the irradiation vessel was connected to the gas samplers of gas chromatographs and the gaseous products were analyzed on 3 m Porapak Q columns. The relative amounts of the products were calculated from peak areas in the gas chromatograms and sensitivities of the products determined previously.

Yellowish white powder formed on the glass plate was collected, weighed and pressed to form KBr disk to be subjected to infrared spectrophotometry on a Hitachi 183 Spectrophotometer. The solubility of the powder was tested against 10 solvents at room temperature. Dose rate absorbed by acetylene was calculated based on the N_2O dosimetry data.

Studies on RF discharge were carried out using a plasma reaction tester manufactured by SAMCO Co. (Type PR-1). The schematic diagram of the reactor is shown in Fig. 1. The discharge chamber is of a glass belljar of 8.91 capacity with two parallel electrodes (top ϕ80 mm, bottom ϕ100 mm in diameter and distance was set at 35 mm). The lower electrode was

covered with aluminium foil to protect its surface from being contaminated with discharge products. Discharge power was in the range from 0.5 W to 10 W and frequency of the RF power was 13.56 MHz.

Acetylene was fed through a flow meter (Kofloc RK-1400) from a tank. The belljar was evacuated by a rotary pump. The highest vacuum attained was 0.1 mm Torr. The pressure in the belljar was measured by a thermocouple gauge (Edwards, Model TC-1).

The RF power was fed to the top electrode, while the bottom electrode was grounded, through a standing wave ratio meter with impedance matching network. The RF power absorbed in the gas was tentatively calculated as the difference between forward and backward power. On the bottom electrode, were placed aluminium deposited glass plates on which thin polymer film is to be deposited by the discharge. The film thickness was monitored by the film thickness gauge[6] with the quartz oscillator sensor which was installed near the lower electrode in the reaction chamber. The output signal from the gauge was recorded on a strip chart recorder as mentioned earlier.

After discharge, the glass plates (50 mm × 3.5 mm, 50 × 30 mm) were taken out to be subjected to thickness measurement by interferometer and to functional group analysis by multiple reflection infrared spectroscopy. The capacitance of the film was measured using a YHP 4262 A LCR meter at 1.0 KHz.

The amounts of products found in the gas phase after irradiation of acetylene were listed in Table 1 together with the G values and reaction conditions. The G value of acetylene consumption was calculated to be 40 on the basis of pressure decrease of acetylene during irradiation.

Yellowish white powder was only form of solid product in electron irradiation and no visible film was found on the glass plate or on the wall of the irradiation vessel. The amount of solid powder was roughly 100 mg, which gives the G value of

acetylene consumption assuming that the solid has $(C_2H_2)_n$ formula.

The G values of the products found in the present study are a little lower than the values reported in the literature,[10] but not much different from these values. The G values of the powder is about a half of that reported for $G(-C_2H_2)$ which is almost equal to that calculated from the

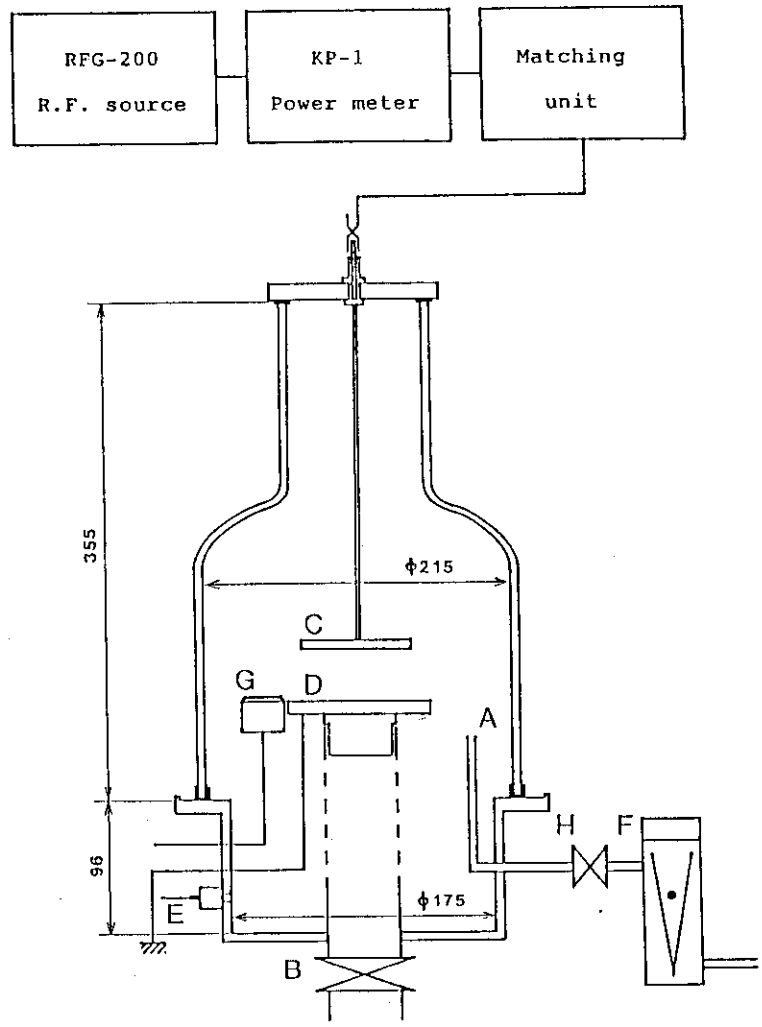

Fig. 1 Plasma reactor; (A)monomer inlet, (B)to vacuum pump, (C)upper electrode, (D)lower electrode, (E)thermocouple gauge, (F)flow meter, and (G)thickness sensor

pressure decrease of acetylene by electron irradiation.

The infrared spectra of the powder are shown in Fig. 2 indicating that the product is hydrocarbon. When the polymer was left in air for several hours, the band of carbonyl group appeared suggesting that oxydation reaction occurred under these conditions (Fig. 2c). Infrared spectra of film and powder obtained by plasma polymerization and electron beam polymerization of acetylene (Fig. 2) showed similar feature each other, in which bands due to stretching vibration and deformation vibrations of CH, CH_2, and CH_3 groups appeared with slight absorption bands due to C = C double bond. These IR spectral features together with the fact that the solid products were insoluble to all solvents tested indicate that the solid product is mainly hydrocarbons with highly cross-linked and saturated. In the IR spectra, the band due to -OH group was also found. The intesity of this band decreased and band due to stretching vibration of -CO-CO- group appeared and its intensity increased when the film was exposed to air. These findings indicate that the -OH group is produced by a reaction of O_2 contained in acetylene as impurity and the -OH groups in the solid products are further oxidized to form diketone by atmospheric oxygen.

The band due to the stretching vibration of C = C group appeared at 1600 cm^{-1} is observed in Fig. 2 but it is weaker for (b) and (c). This band is very strong in the spectrum (d). These observations suggest that polymer obtained from acetylene contains more double bonds than that prepared from methane or ethane as noted by Kobayashi, Bell, and Shen,[9,11] but the double bond is the most abundant in the polymer obtained from C_2H_4.

Polyacetylene obtained by catalytic polymerization (Fig. 2f) shows IR spectrum completely different from that observed for polymerized acetylene (Fig. 2d) indicating that the film obtained from acetylene by discharge does not contain conjugated double bond. The pressure and temperature in the

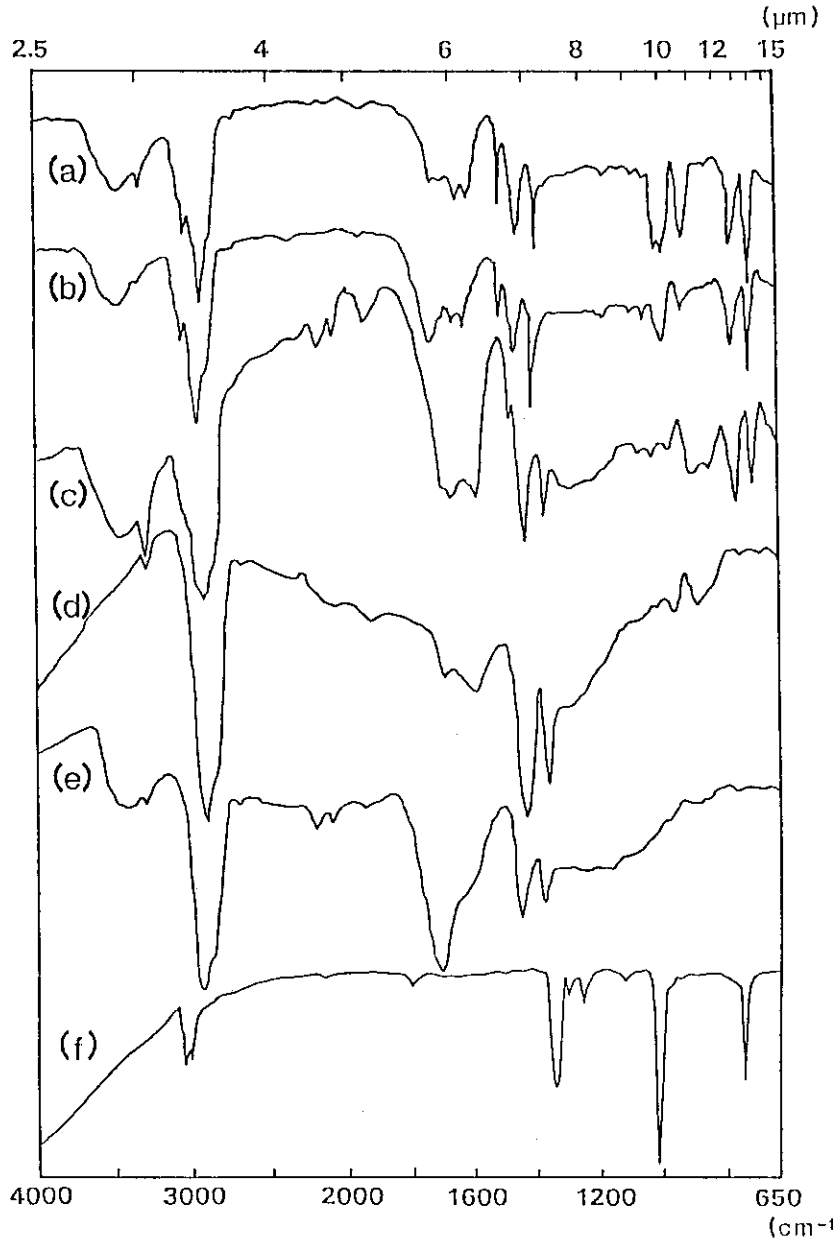

Fig. 2 Infrared spectra of film and powder of acetylene;
(a)powder obtained by electron beam polymerization,
(b)the same as (a) after 5 days in air,
(c)powder obtained by plasma polymerization,
(d)film obtained by plasma polymerization,
(e) the same as (d) after 10 days in air, and
(f) poly-acetylene prepared by catalytic polymerization (H. Shirakawa and S. Ikeda, Polym. J., 2, 235 (1971).

vessel during irradiation were plotted as a function of time in Figs. 3 and 4 for the initial reaction pressures of 170 Torr and 18 Torr, respectively; the pressure change corrected for that due to the temperature change during irradiation is also shown in the same figures. The plots of the reciprocal of the corrected pressure as a function of reaction time lie on a straight line as shown in Fig. 5. This result indicates that the reaction proceeded with second order reaction and the reaction constant was estimated to be $6.82 \times 10^{12} \cdot \text{molec}^{-1} \cdot \text{sec}^{-1}$ from the slope of the plot.

The powder which was accumulated on the film thickness sensor did not give any response to the output of the film thickness monitor, but film formed on the sensor did give output. An example of the output signal from the film thickness monitor as a function of time is shown in Fig. 6.

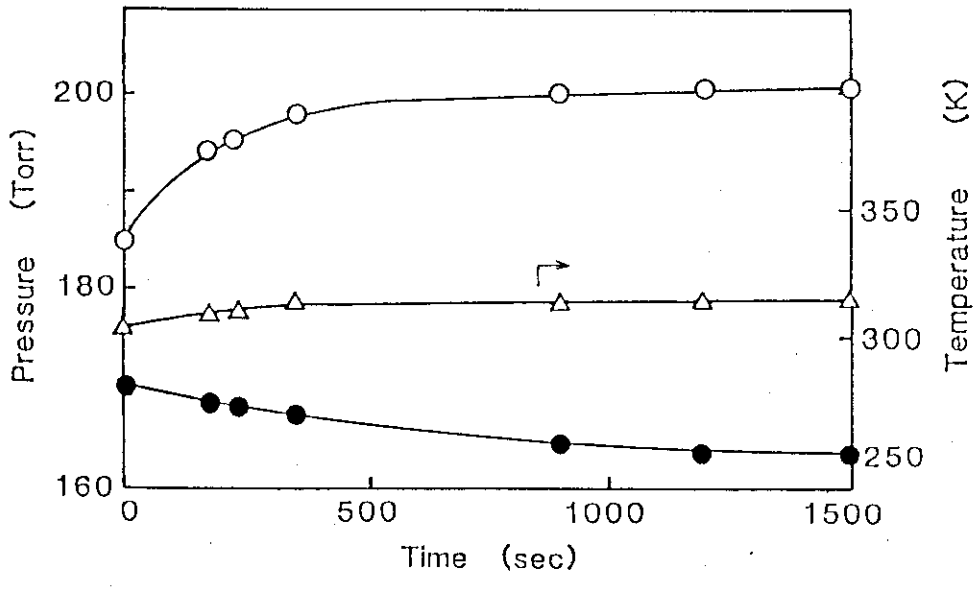

Fig. 3 Pressure as observed (o), pressure after corrected with temperature (o), and temperature ( ) as a function of irradiation time.

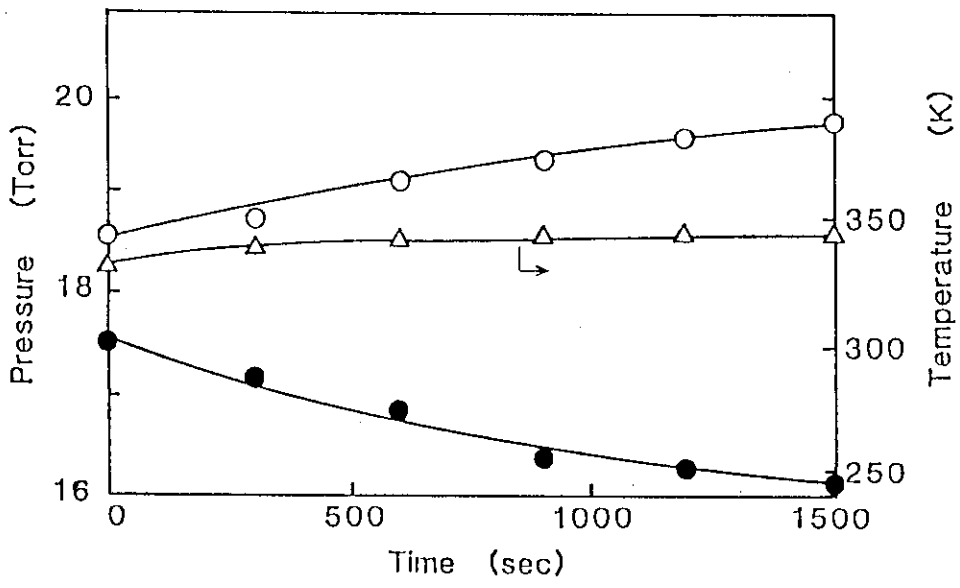

Fig. 4 Pressure as observed (o), pressure after corrected with temperature (o), and temperature ( ) as a function of irraddiation time.

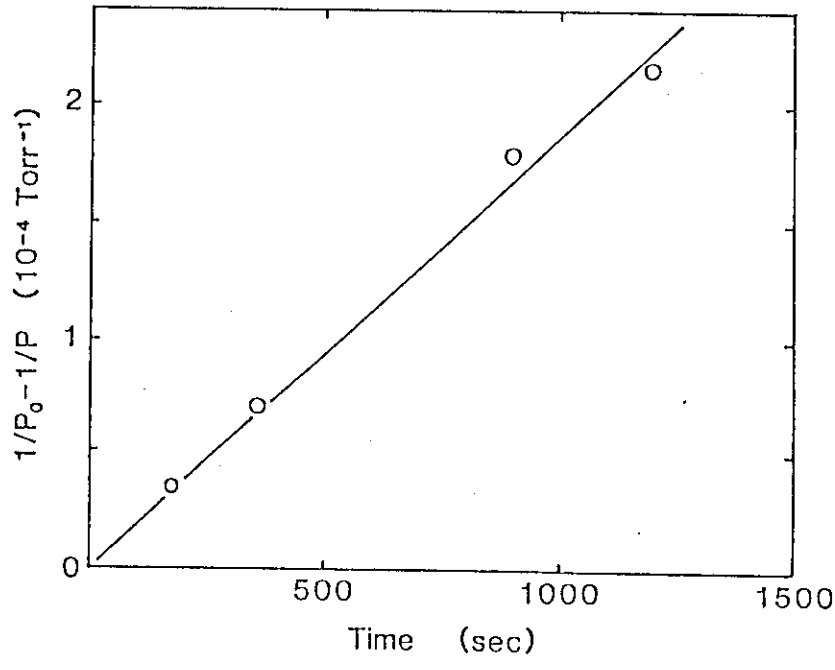

Fig. 5 Second order kinetics plot.

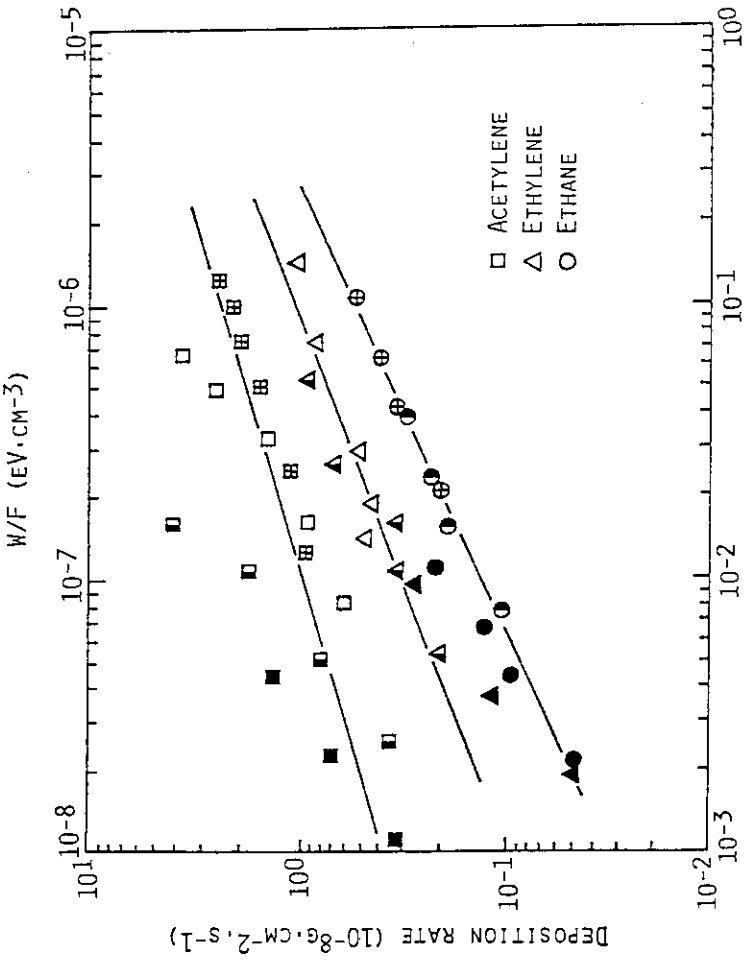

Fig. 7 Film deposition rate as a function of W/F falues; pressukre (in Torr): crossed, 0.034; blank, 0.045; right half filled, 0.075; left half filled, 0.098; and filled, 0.18.

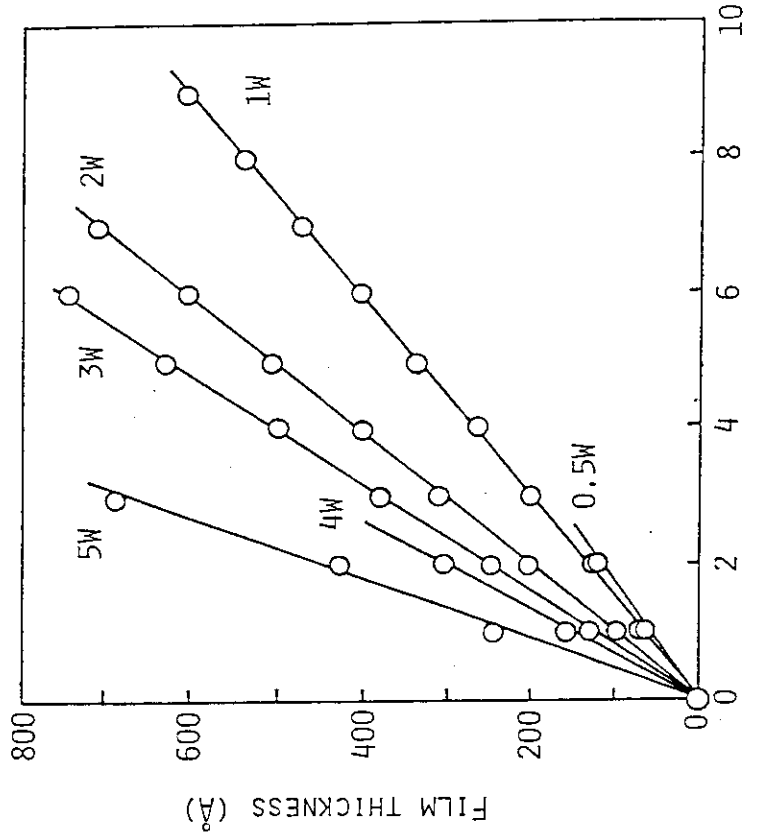

Fig. 6 Film thickness as a function of discharge time; pressure, 0.034 Torr; gas, acetylene.

The plots show that the film thickness increases with discharge time in the time range studied.

The RF power to flow rate ratio or RF power to pressure ratio may be taken as an indication which relates to power absorbed by a molecule. The plot of deposition rate was plotted as a function of the power to pressure ratio for different compounds in Fig. 7. The deposition rate is higher for the molecules of higher unsaturation.

Since the plasma reactions were carried out under low gas pressure below 10 Torr where gas analysis was difficult to perform, no information was obtained for gaseous products.

Solid products were formed either in the form of yellowish thin film or in that of white powder depending on the reaction conditions employed. Fig. 8 shows the map which indicates which type of solid products were formed under the pressure and

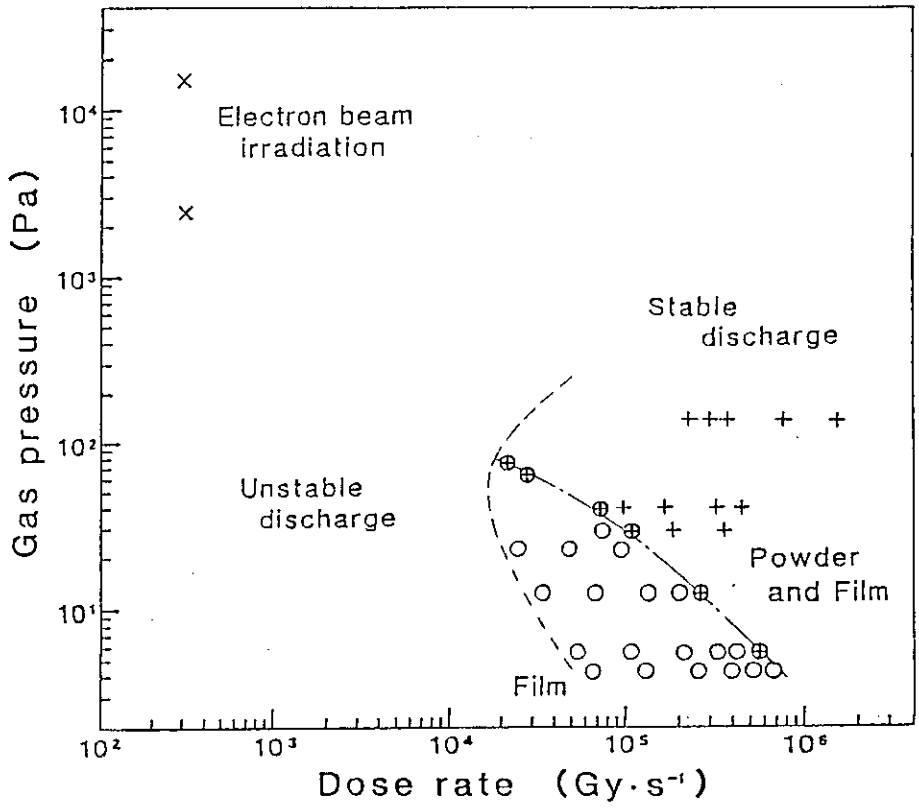

Fig. 8 Characteristic map kfor the plasma polymerization of acetylene.

Table 1 G-values

P(Torr)	$G(-C_2H_2)$	$G(C_2H_2)_n$	$G(C_6H_6)$
17.5	41.9	----	---
116*	66.8	----	5.6
135	39.8	24.5	0.8
145*	65.5	----	3.5

*) by L. M. Dorfman[10)]

electric power employed. The powder is favorably formed at high gas pressure and high RF power, while film usually appeared when the discharge reaction was performed at low pressure. Similar observations were made by Kobayashi, et al., for the discharge chemistry of ethylene.[9)]

The pressure-dose rate condition employed for the electron beam irradiation experiments in which only powder was obtained came to the point above the extention of the line which separates the film forming zone from the powder forming one. Therefore, it is expected that the products in film form will also be obtained by the electron beam irradiation if the irradiation is carried out at low pressure which are indicated by a point below the line or its extention. The capacitance and resistance of the film obtained from acetylene by RF discharge were 1.7 nF and 5.2M , respectively.

(M. Hatada, T. Kijima, and N. Kawakami)

1) W. Mund and W. Koch, J. Phys. Chem., 30, 389 (1926).
2) L. M. Dorfman and F. J. Shipko, "The -Particle Radiolysis of Acetylene", J. Am. Chem. Soc., 77, 4723 (1955).

3) H. Yasuda and T. Hirotsu, "Critical Evaluation of Conditions of Plasma Polymerization", J. Poly. Sci. :Poly. Chem. Ed., 16, 743 (1978).
4) H. Kobayashi, A. T. Bell, and M. Shen, "Plasma Polymerization of Saturated and Unsaturated Hydrocarbons Macromolecules", 7, 277 (1974).
5) S. Sugimoto, M. Nishii, and T. Sugiura, "Radiation Chemistry of CO-H_2 Gas", JAERI-M 7898 (1978).
6) H. Yasuda and N. Inagaki, "The Initial and Termination Stage of Glow Discharge Polymerization Investigated by Thickness Monitor", J. Appl. Polym. Sci., 26, 3557 (1981).
7) H. Suzuki, T. Fujii, and K. Koyama, "Interpretation of IR-Spectrum", Kagaku Chemistry, 38, 1 (1983).
8) H. Kobayashi, A. T. Bell, and M. Shen, "Structural Characterization of Plasma-Polymerized Hydrocarbons", J. Macromole. Sci. : Chem., A10, 1623 (1976).
9) H. Kobayashi, A. T. Bell, and M. Shen, "Effects of Reaction Condition on Plasma Polymerization of Ethylene", J. Macromole. Sci. : Chem., A8, 373 (1974).
10) L. M. Dorfman and A. C. Wall, "The Radiation Chemistry of Acetylene", Radiation Research, 10, 680 (1959).
11) H. Kobayashi, A. T. Bell, and M. Shen, "The Role and Halogens in the Plasma Polymerization of Hydrocarbons", J. Macromole. Sci. : Chem., A8, 1345 (1974).
12) Higashiura and M. Oiwa, Kogyokagaku Zashi, 69, 109 (1966).

6. Reduction of Crystalline Units of Nylon 66 Film by Electron Beam-Irradiation Studied by Melting Point Measurement

Studies have been carried out in an attempt to prepare polymer substrates of different surface morphologies on which thin layer grafting are to be carried out. It is of interest to know the relation between the morphology of the grafting layer and that of the substrate surface. The grafting rate is also expected to depend on the surface morphology of the substrate.

This year we irradiated nylon 66 film with electron beam at different temperatures and studied the changes of the amount of crystalline units and of the length of the crystallite of the film by differential scanning calorimetry. The sample film of nylon 66, 40 μm thick, was obtained from Toray Co. The degrees of crystallinity of the film were low as 29% and 26%, which were evaluated from the heat of fusion and absorbance of 1145 cm^{-1} amorphous band of the infrared spectrum, respectively. Infrared spectrum of the film did not indicate 1329 and 1224 cm^{-1} bands[1] which represent the existence of a folded-chain structure of nylon 66. From the diffuse reflections at 3.98 and 4.23 Å on the X-ray diffraction diagram of the film, nylon 66 molecules are allowed to rotate around the chain axes and are considered to constitute a hexagonal close-packing structure.[2]

Irradiation of the film was performed in a nitrogen atmosphere by the electron beams from a Van de Graff accelerator (1.5 MV, 50 μA, 0.124 Mrad/sec). Irradiation temperatures were 70°C and 26°C which are above and below the glass transition temperature of the film (42°C), respectively.

The observed melting temperature (Tm) of the film irradiated at 70°C was depressed linearly with the increase of the dose. A depression of the melting temperature by irradiation was estimated to be 0.20°C/Mrad from the slope of the linear least square line of the melting point- dose data.

Table 1 Percent gel fraction in irradiated nylon 66 film

Irrad. temperature(°C)	Dose(Mrad)	Gel fraction(%)
70	8.3	0.85
	16.5	26.3
	33.1	60.7
	49.6	69.1
	66.1	75.7
	99.2	75.5
26	16.5	14.6
	33.1	48.0
	49.6	53.3
	66.1	61.3
	99.2	67.6

On the other hand, a depression of the melting temperature of 0.15°C/Mrad, was obtained from the data obtained for the film irradiated at 26°C in the same dose range.

The glass transition temperature (Tg) of the films increased to 47°C and 44°C, when the films were irradiated at 70°C and 26°C, respectively, with the dose of 99 Mrad, suggesting that the cross-linking of the polymer occurred by the irradiation. Percent gel fraction of the irradiatd film was determined by using 2, 2, 2-trifluoro ethanol as a solvent and the result was given in Table 1.

The crystal of the polymer is destroyed to various degrees and becomes amorphous in part because of the cross-linking and the scission of the polymer chain induced by the irradiation. The mole fraction of crystalline units, X can be estimated from

the equation derived by Flory:[3,4]

$$\frac{1}{T_m} - \frac{1}{T_m^\circ} = -\frac{R}{\Delta H_m} \ln X \qquad (1)$$

Where, T_m denotes melting temperature of the sample (K), T_m° equilibrium melting temperature (K), R gas constant (8.314 J mol^{-1} K^{-1}), and ΔH_m heat of fusion (J mol^{-1}). The melting temperature is related to the length of crystallite ℓ (in cm) of the polymer crystal by eq.2.[4,5]

$$T_m = T_m^\circ \left(1 - \frac{2\sigma_e}{\Delta Hm \cdot \ell}\right) \qquad (2)$$

Where σ_e denotes surface free energy of crystallite (J cm^{-2}), and ΔH_m heat of fusion (J cm^{-3}). The changes of the mole fraction of crystalline units and the length of

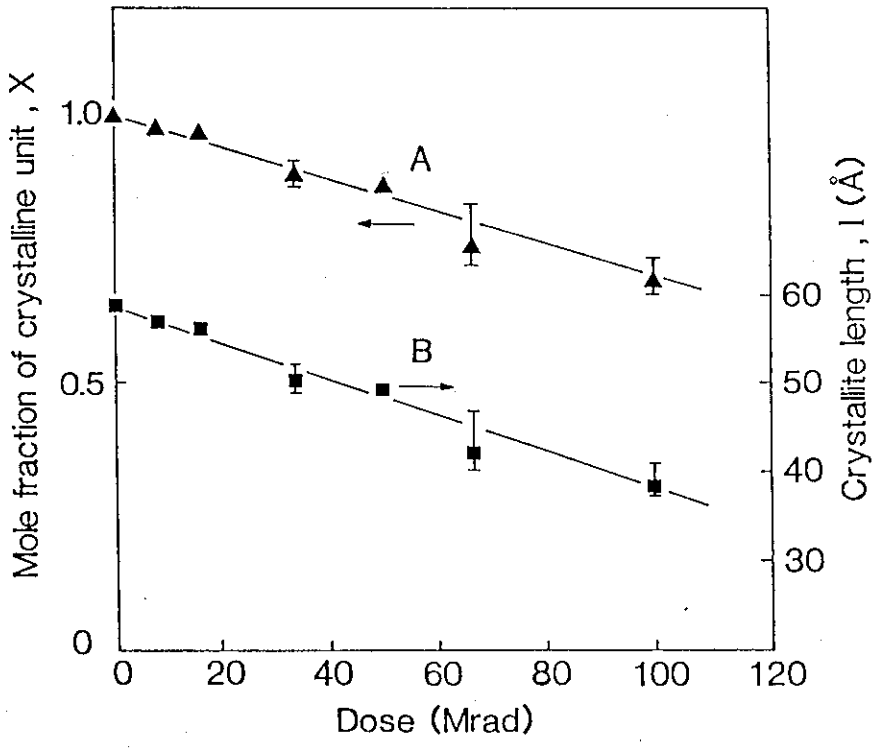

Fig. 1 Dependences of mole fraction of crystalline unit (X) and crystallite length (ℓ) on doses in nylon 66 irradiated at 70°c.

crystallite with irradiation were calculated using eq. (1) and (2), respectively, using the values reported by Takemori, et al.,[6] i,e., T_m° = 567 K, ΔH_m = 4.26 × 10^4 J mol^{-1} (= 2.33 × 10^2 J cm^{-3}), and σ_e = 4.40 × 10^{-6} J cm^{-2}. The mole fraction of crystalline units in the film irradiated at 70°C decreased linearly with the increase of the dose to 0.69 at the dose of 99 Mrad (Fig. 1), while the mole fraction of crystalline units decreased to 0.75 at the same dose when the irradiation was carried out at 26°C (Fig. 2). The length of crystallite of the film also decreased linearly with increasing dose as shown in the same figure: The length of crystallite of the film decreased from 59 Å to 38 Å when the irradiation was carried out at 70°C at 99 Mrad, whereas the length of crystallite of the film decreased to 42 Å when the irradiation was carried out

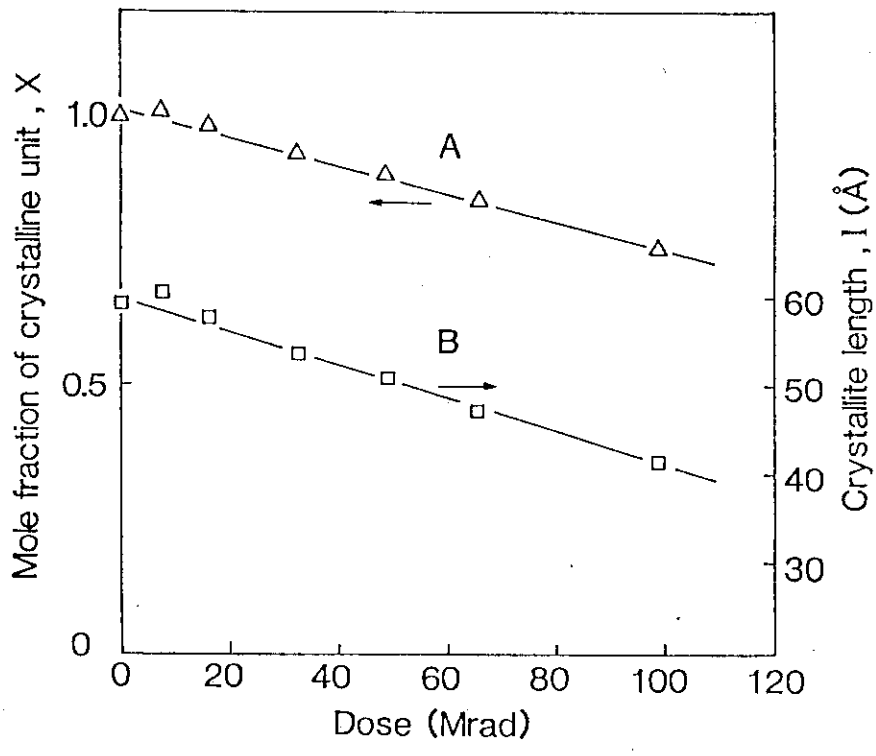

Fig. 2 Dependences of mole fraction of crystalline unit (X) and crystallite length (ℓ) on doses in nylon 66 irradiated at room temperature.

at 26°C at the same dose.

The results that the decrease of the mole fraction of crystalline part is accompanied with the decrease of the length of the crystallite indicate that the cross-linking and chain scission of nylon molecules occur in the crystalline part resulting in the destruction of the crystallites. Similar experiments on high density polyethylene film carried out for comparison to the above results indicate that mole fraction of the crystalline part and the length of crystallite decreased to 0.98 and 61 Å, respectively, by the irradiation at 86°C at 30 Mrad but did not change when the irradiaion was further carried out up to the dose of 93 Mrad. The conclusion derived from these results combined together is that little collapse of crystalline lattice occurred in high density polyethylene crystallite as is generally accepted[7], whereas significant collapse of the crystal lattice occurred in nylon 66 film, possibly due to the existence of a disorder around the chain axis (of the polymer molecule) which may disturb the network of interchain hydrogen bond.

(M. Nishii)

1) J. L. Koenig and M. C. Agboatwalla, J. Macromol. Sci. - Phys. Ed., B2, 391 (1968).
2) I. Sandeman and A. Keller, J. Polym. Sci., 19, 401(1956).
3) M. Dole and W. H. Howard, J. Phys. Chem., 61, 137 (1957).
4) L. Mandelkern, "Crystallization of Polymers", McGraw-Hill New York, 1964, chapter 4.
5) A. Nakajima and M. Hosono, "Molecular Physics of Polymers", Vol. II, Kagakudozin, 1969, P. 453.
6) H. Takemori, K. Miyasaka, and K. Ishikawa, Sen-i Gakkaishi, 26, 74 (1970).
7) M. Dole, ed., "The Radiation Chemistry of Macromolecules", Vol. I, Academic Press, New York, 1972, P.

7. Improvement of Adhesive Strength at Polyvinylchloride-Polyester Interface by Radiation-Induced Grafting of Acrylonitrile onto Polyester Filaments

In order to improve the strength of Polyvinylchloride sheet reinforced by polyester fibers, studies were carried out on the modification of surface of polyester fiber to give compatibility to poly (vinyl chloride) by radiation-induced surface grafting technique. Acrylonitrile(AN) was selected as monomer to be grafted, since AN has a large co-solublity with polyvinylchloride.

Polyester mono filament used in the present study was of 30 denier. AN was used after distillation to remove inhibitor. Ethylene dichloride (EDC) of reagent grade was used as a swelling agent as supplied by Nakarai Chemicals Co.

Most grafing experiments were carried out using simultaneous irradiation technique on filaments immersed in the monomer. Typical experimental condition is that 0.1 g of polyester filament was added with 4 ml AN-EDC mixture in a glass ampoule (1cm diameter) and the mixture was deaerated by bubbling nitrogen stream for 2 min and then the glass ampoule was sealed. The irradiations were carried out with Co 60 gamma-rays at room temperature. After irradiation, the filament was immersed in DMF to extract out AN homopolymer, washed with water and ethanol, and then dried under vacuum for weighing the filament. The graft-percent was calculated from the weight increase.

Mechanical properties of the filament, adhesive strength to polyvinylchloride, mechanical properties of polyester filament reinforced plyvinyhlchloride were measured by the methods which will be described later.

Table 1 shows the graft-percent as a fuction of dose rate in the range from 6.2×10^3 rad/h to 1.7×10^5 rad/h when AN-EDC (2 : 1 by volume) mixture was used as a monomer solution. Homopolymer solid of AN was found in the ampoule

Table 1 Grafting of acrylonitrile onto polyester fiber at different dose rate.
acrylonitrile: ethylene dichloride = 2 : 1(by vol.)

Dose rate (rad/h)	Irrad. time (h)	Graft (%)	Appearance of monomer soln. after irradiation
1.7×10^5	1	6.5	Solid (hard)
	3	11.7	
9.3×10^4	1	3.4	turbid soln.
	3	8.2	solid (hard)
	7	12.3	
2.6×10^4	3	5.7	solid (hard)
	7	8.3	
6.2×10^3	7	5.2	turbid soln.
	16	6.2	slid (soft)

after irradiation even at the graft-percent as low as 6 %. The dose rate dependence of the rate of grafting determined from the initial slope of the time-conversion curve was found to be 0.75th power of the dose rate which is between 0.7 and 0.8 reported for the bulk polymerization of AN.[1)]

The graft-percent was plotted as a function of monomer content in the mixture at 3 and 7 h after initiation of the grafting at 9.3×10^4 rad/h in Fig. 1. As shown in the figure, the graft-percent increased with increasing content of AN in the monomer solution and sharply increased when the AN content exceeded 80 %. The homopolymer was formed as suspension in the monomer mixture at AN content of 40 %, but was formed in solid at AN contents above 60 %. Therefore, the AN contents between 40 and 50 % are recommended for the grafting at reasonable rate of grafting with possible minimum amount of homopolymer formation.

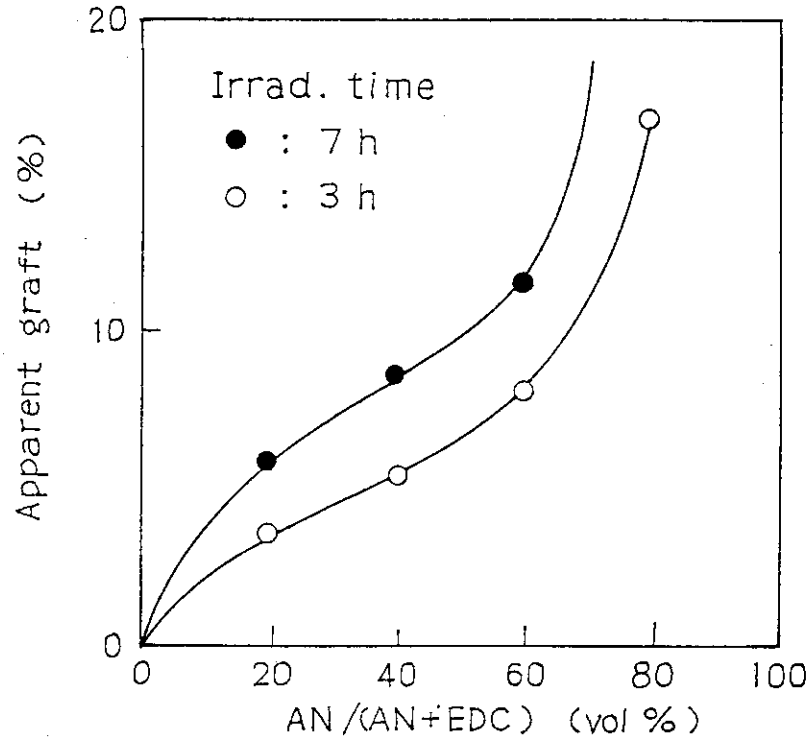

Fig. 1 Effect on monomer concentration on the grafting of acrylonitrile onto polyester fiber. Dose rate: 9.3×10^4 rad/h.

Table 2 Tensile properties of acrylonitrile graft polyester fiber

Graft (%)	Denier (d)	Strength (g)	Tenacity (g/d)	Elongation (%)
0	29.7	135	4.5	98
8.2	32.1	146	4.5	110
8.6	32.3	137	4.2	85
11.6	33.1	144	4.4	120
11.7	33.2	144	4.3	100
12.5	33.4	136	4.1	80
18.8	35.3	145	4.1	100

Table 2 lists the experimental results of the strength and elongation measurements on AN graft polyester fiber using an Instron tensile tester at 23°C and 65 % relative humidity. Strength and elongation of the filament did not change by the grafting. Tenacity apparently decreased but this is due to an increase of denier of the fiber by the grafting. Thus, the excellent mechanical properties of the original polyester filament were not lost by the radiation-induced grafting.

Preliminary test of the adhesive strength was carried out using the Instron tensile tester on the test specimens which were prepared by the following method: two parallel polyester filaments were placed on a sheet of polyvinyl chloride film prepared from polyvinylchloride sol by heat-curing, they were covered with polyvinylchloride sol, and then the whole composite was heat-cured at 170°C for 5 h. The two filaments

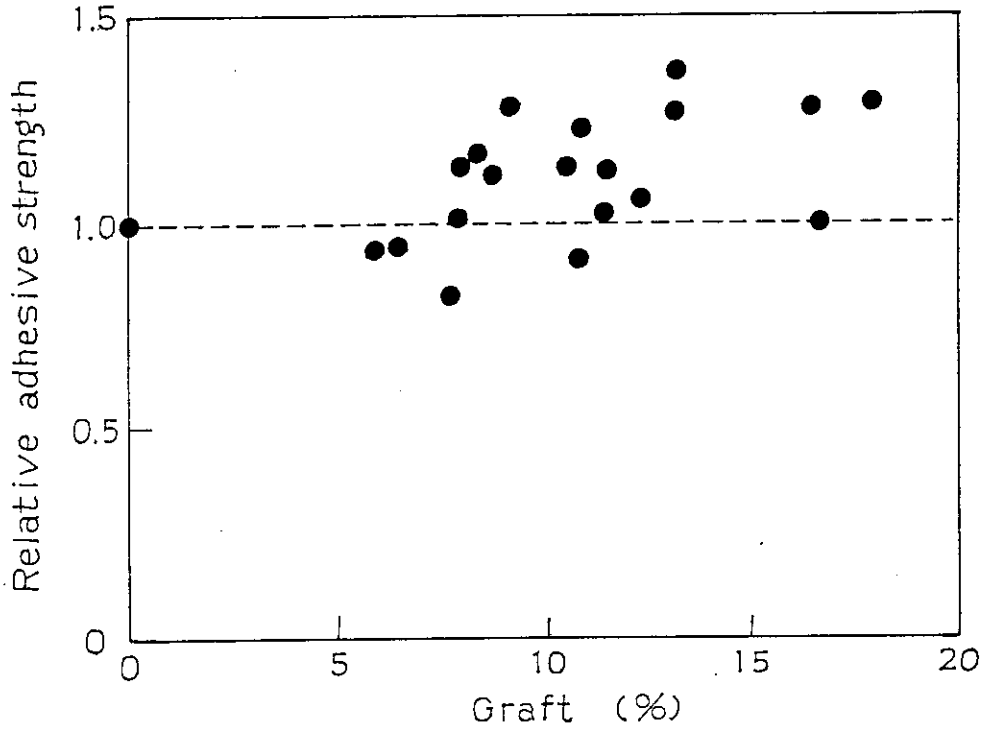

Fig. 2 Adhensive strength versus graft percent for the acrylonitrile graft polyester fiber.

were pulled in opposite directions each other by the Instron tensile tester at 1 cm/min, and the force at which the filament is pulled out from the specimen is taken as the adhesive strength.

The relative adhesive strength of the grafted filament, which is normalized to the adhesive strength for the original one as unity, is plotted as a function of the graft-percent in Fig. 2, which shows the adhesive strengths for the grafted filaments above 8 % graft are higher than the original one, though the points are scattered possibly because the surface concentration of AN and suface structure of the filament are the factors to govern the adhesive strength, which will need further considerations in the future studies.

(K. Kaji)

1) A. Chapiro, "Radiation Chemistry of Polymer System" Interscience Pub., N. Y., P. 205.

Ⅲ. LIST OF PUBLICATIONS

[1] Published Papers

1. K. Matsuda, T. Takagaki, Y. Nakase, and Y. Nakai, "The Radiation Shielding and the Dose Distribution for the Building of the High Dose Rate Accelerator", JAERI-M 84-057 (1984).

2. N. Fukuoka, Y. Kanbe, H. Saitoh, and K. Matsuda, "Irradiation Induced Deffects Containing Oxygen Atoms in Germanium, Crystals as Studied by DLTS", JAERI-M 84-091 (1984).

3. M. Hatada, "Polymerization of Monomers in a Form of Built-up Multilayer films and Application of the Polymerized Multilayers", Polymer Digest, 36, 7 (1984).

4. S. Nagai, H. Arai, and M. Hatada, "Role on Silica Gel in the Radiation-Induced Reaction of CO/H_2 Gas Mixture", Nihon Kagaku kaishi (1984) P 1656.

5. S. Nagai and Y. Shimizu, "SIMS Study on Ion Impact Desorption of Water from Silica Gel", in Secondary Ion Mass Sepectrometry, SIMS IV, ed. by A. Benninghoven et al. (Springer-Verlag, 1984), p 463.

6. S. Nagai and Y. Shimizu, "Electron and Ar^+ Ion Impact Effects on SiO_2, Al_2O_3 and M_gO", J. Nucl. Mat., 128/129, 605 (1984).

7. T. Oshiyama, S. Nagai, K. Ozawa amd F. Takeuchi, "Data Compilation for Particle Impact Desorption", JAERI-M 84-094 (1984); J. Nucl. Mat., 128/129, 996 (1984).

8. M. Hatada and K. Matsuda, "SIMS-Auger Analysis of Organic Films on Gallium Arsenide", in Secondary Ion Mass Spectrometry, SIMS IV, ed. by A. Benninghoven et al. (Springer-Verlag, 1984), p 225.

9. S. Sugimoto, M. Nishii, and T. Sugiura, "Radiation-Induced Chemical Reaction of Carbon Monoxide and Hydrogen Mixture 1. Electron Beam Irradiation at Atmospheric Pressure", Radiation Physics and Chemistry, 24, 567 (1984).

10. K. Kaji, "Radiation-Induced grafting of Acrylic Acid onto Polyester Fiber" Industrial and Engineering Chemistry, Product Research and Development, 24 (1985).

11. K. Matsuda, Y. Nakase, Y. Tsuji, and I. Kuriyama, "Effect of Atmosphere on the Thermolumilnescence of Irradiated Polyethylene", Reports on Progress in Polymer Physics in Japan, 27 (1984).

12. S. Sugimoto and M. Nishii, "Radiation Induced Chemical Reaction of Carbon Monoxide and Hydrogen Mixture. The Increase in the Yields of Oxygen Containing Products by Addition of Methane", JAERI-M 84-224 (1984).

[2] Oral Presentations

1. S. Sugimoto, M. Hatada and S. Nagai "Surface Structure and Catalytic Activity of Silicon and Silica-gel Surface Modified by Electron Beam Recoil Doping of Iron", 37th Discussion Meeting on Colloid and Surface Phenomena (Morioka), Oct. 1, 1984.

2. Y. Shimizu, S. Nagai, and M. Hatada, "Structurue and Decomposition of the Carbonaceous Solid Produced on the Surface of Molecular Sieve 5A by Irradiation of Methane", 27th Discussion Meeting on Radiation Chemistry (Tokyo) Oct. 3, 1984.

3. S. Nagai and Y. Shimizu "Electron and Ar^+ Impact Effects on Alumina" 27th Discussion Meeting on Radiation Chemistry (Tokyo), Oct. 3, 1984.

* * * * * *

4. S. Nagai, "Adsorption of CO and CO_2 on the Surface of Alumina under Electron Impact", Japan Society for The Promotion of Science, The 141st Committee, 32nd Symp. (Osaka), Dec. 5, 1984.

5. S. Nagai, " Utilization of Electron Beams in the Study of Petrochemistry", Japan Oilchemists' Society, Kansai District Soc., 26th Lecture Meeting, (Osaka), Jan. 25, 1985.

Ⅳ. EXTERNAL RELATIONS

A training program for scientists and engineers in industries and government organizations was held in the laboratory as one of the courses offered by the Radio-isotope school, JAERI in Tokyo. This one week program starting Oct. 22 included lectures and laboratory experiences concerned with the radiation chemistry of polymers from its basic subjects to recent application in industries. We welcomed 13 trainees this year.

Some studies in this laboratory were conduced under the cooperative agreements with Prof. Y. Tsuji of Kinki University, Prof. H. Saito of Osaka University. A sponsored investigation was made under the contract with the Mitsubishi Electric Corporation.

Dr.R. M. Iyer of Bhabha Atomic Energy Research Centre visited on Nov. 21 to deliver lectures on the recent advancement in the Chemistry Division of the Institute and to discuss studies on radiation chemistry of simple gases under the presence of solid catalysts.

V. LIST OF SCIENTISTS
(March 31, 1985)

[1] Staff Members

Motoyoshi HATADA	Dr., physical chemist, Director
Seizo OKAMURA	Professor emeritus, Kyoto University
Siro NAGAI	Dr., physical chemist
Shun'ichi SUGIMOTO	Physical chemist
Koji MATSUDA	Radiation physicist
Jun'ichi TAKEZAKI	Physical chemist
Masanobu NISHII	Dr., polymer chemist
Torao TAKAGAKI	Radiation physicist
Kanako KAJI	Dr., polymer chemist
Yuichi SHIMIZU	physical chemist